Synthesis of Nd:YAG Nanopowder for transparent ceramics

A thesis submitted in partial fulfillment of the

requirements for the degree of

Bachelor of Technology

in

Ceramic Engineering

By

Apurv Dash

(Roll No- 109CR0660)

Under the guidance and supervision of

Prof. Debasish Sarkar

Department of Ceramic Engineering

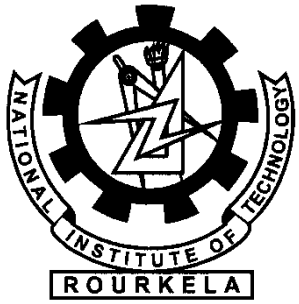

Department of Ceramic Engineering

National Institute of Technology, Rourkela

2013

National Institute Of Technology

Rourkela

CERTIFICATE

This is to certify that the thesis entitled, "**Synthesis of Nd:YAG Nanopowder for transparent ceramics"** submitted by **Apurv Dash (109CR0660)** in partial fulfillment of the requirements for the award of Bachelor of Technology in **Ceramic Engineering** at the National Institute of Technology, Rourkela is a bonafide research work carried out by him under my supervision and guidance. To the best of my knowledge, the matter embodied in the thesis is based on candidate's own work, has not been submitted to any other university / institute for the award of any degree or diploma.

Date:

Supervisor

Prof. Debasish Sarkar
Dept. of Ceramic Engg.
National Institute of Technology
Rourkela – 769008

Acknowledgement

With deep regards I wish to thank Prof. S.K. Pratihar who has supported me throughout my project in terms.

I avail this opportunity to extend my heartfelt thanks to my guide Prof. D. Sarkar, Ceramic Engineering for his generous sharing of wisdom, magnificent support, constant encouragement and never ending patience throughout the entire period of investigation.

I would like to express my deepest gratitude and heartfelt regards to Prof. H.S. Maiti to invest confidence in me to take up a real time venture for my final year project.

Thanks for your love and support!

I extend my deep sense of gratitude to Dr. Ashim kumar Chakrobaty (Chief scientist & Head) of Central Glass and Ceramic Research Institute, Kolkata for necessary characterization of the nanopowders.

I would also like to thank Dr. Byung Nam Kim (Chief researcher, Advanced Ceramics Group) of National Institute of Material Science (NIMS), Japan for spark plasma sintering of YAG nanopowders.

I thank Ms Sangeeta Adhikari to help me perform experiments in the laboratory.

A part of thanks is due for my parents, sister, brother-in-law and Pragya who were always by my side and whose support knows no limit.

Apurv Dash

Contents

List of Figures

List of Tables

List of abbreviations

SSL	Solid State Laser
HEL	High Energy Laser
LASIK	Laser Assisted In-Situ Keratomileusis
PCO	Posterior Capsulotopy Opacification
YAG	Yttrium Aluminium Garnet
SP	Scattering (pore)
SSP	Scattering (secondary phase)
SOA	Scattering (optical anisotropy)
YAM	Yttrium Aluminium Monoclinic
YAP	Yttrium Aluminium Perovskite
CIP	Cold Isostatic Pressing
SPS	Spark Plasma Sintering
HIP	Hot Isostatic Pressing
TEM	Transmission Electron Microscopy
TEOS	Tetra Ethyl Ortho Silicate
FTIR	Fourier Transform Infrared Spectrocsopy
BET	Brunauer -Emmett -Teller
UV-VIS	Ultraviolet-Visible Spectroscopy
DSC	Differential Scanning Calorimeter
TG	Thermo-gravimetry
XRD	X-ray Diffractometer
DLS	Dynamic Light Scattering
EDS	Energy Dispersive Spectroscopy

Abstract

Current trend on high energy laser is now the booming field of research, because of the continuous increase in the power output such as 100 KW. The increase in power output is due to increase in active ion concentration and size of the laser host material. The current work is based on the synthesis of Yttrium Aluminium Garnet (YAG-$Y_3Al_5O_{12}$) nanopowders for the fabrication of transparent ceramic laser gain media. YAG nanopowders have been prepared by co-precipitation route by using Aluminium nitrate and Yttria as starting precursor and precipitated against ammonium bicarbonate at low temperature (10 ^{o} C) and pH 7.3. All the subsequent washing and freeze drying processes to obtain agglomerate free powder are carried out at 10 ^{o} C and -52 ^{o} C, respectively. The as-precipitate agglomerate free powder is further calcined in the temperature range from 900 to 1100 ^{o} C. The powder calcined at 900 ^{o} C is highly reactive with a particle size below 50 nm and surface area of 42 m^2/gm. The calcined powders are doped with silica, consolidated through uniaxial pressing and followed by atmospheric pressure-less sintering at 1650 ^{o} C for 6 hr. Sintering profile has been optimized on the basis of achieved ρ_{rel} ~ 99% and further proceed for spark plasma sintering with addition of 5at.% Nd dopant concentration. The spark plasma sintering process is carried out at 1300 and 1400 ^{o} C for 5 minutes with a uniaxial loading of 62 MPa. Optical transparency of spark plasma sintered disc specimen is rendered transmission of 30 % in the infrared range and 10 % in the visible range.

Keywords: Nanopowder; Yttrium Aluminium Garnet (YAG); Spark Plasma Sintering (SPS); Transparent ceramics.

Chapter 1

Introduction

Chapter 1

Introduction

Solid state laser based on ruby as the laser gain material was first demonstrated in 1960 using a xenon flash light pumping system [1]. The main criteria of a laser gain material is transparency in the visible as well as infra-red region, which is the main challenge researchers are facing in the present scenario. Lasers have played an important role in revolutionising the scientific as well as industrial sector. Solid state lasers (SSL) have successfully been used in strategic as well as civilian sectors. The applications of SSL include laser assisted in-situ keratomileusis (LASIK), high energy laser weapons (HEL), posterior capsulotopy opacification (PCO), industrial welding, engraving, Raman spectroscopy and many more.

While the most commonly used solid state laser gain material used in industry is the single crystal of Yttrium Aluminium Garnet (YAG) doped with Nd^{3+} popularly known as Nd-YAG, the current trend is to use transparent polycrystalline YAG ceramics replacing the single crystals primarily because of economic consideration. For obvious reasons, polycrystalline transparent ceramics have a different route of fabrication.. The criteria [2] which need to be fulfilled for a polycrystalline ceramic material to be transparent are:

- The sintered density should be very high (close to theoretical) and the body should be absolutely free of any residual porosities.
- The material should also be free of secondary phases such as inclusions, inter-granular films or pores and composed a of single phase.
- Grain size is a matter of concern if the crystallography of the system is non-cubic, the grain size should be in sub-micron range.

- The band gap of the material should be more than the energy of quanta of visible light.

Transparent ceramics is a class of advanced functional materials which has a unique combination of mechanical and optical transmission properties. When electromagnetic radiation falls on a transparent sintered body it undergoes many phenomenon such as reflection, refraction, absorption due to non-homogeneity and finally gets transmitted through the other side of the sintered body. Grain boundary, the second phase inclusions and rough surfaces and pores are the main sources of scattering and absorption of light in polycrystalline material [3]. Absorption coefficient of a material is given by $\mu = SP + SSP + SOA$, where SP, SSP, SOA are scattering terms for pores, secondary phases and optical anisotropy respectively. When the photons in the incident beam of the electromagnetic radiation interacts with materials, optical absorption takes place resulting in lattice vibration or excitation of electrons between energy levels. The figure demonstrates scattering due to various phenomenon.

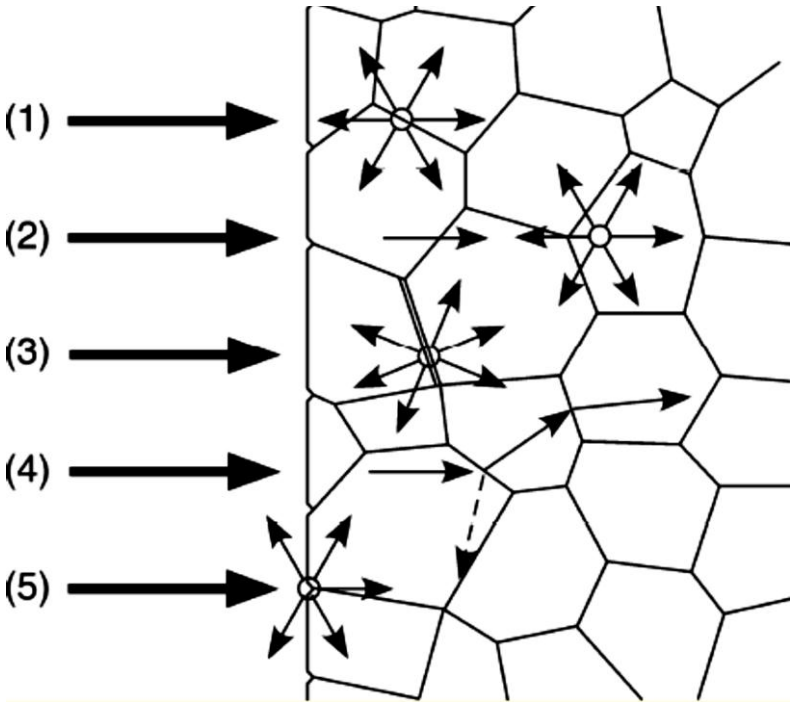

Figure 1.1 Interaction of light with polycrystalline ceramics.

The schematic shows different factors due to which scattering losses occur during interaction with light rays. The factors include (1) grain boundary scattering, (2) inclusion or pore scattering, (3) secondary phase scattering, (4) change in refractive index across the grain boundary and (5) surface scattering, as shown in Figure 1.1.

A Variety of materials are under investigation for transparent ceramics application. Some of the common ceramics include Yttium aluminium garnet ($Y_3Al_5O_{12}$), alumina (Al_2O_3), zinc sulphide (ZnS), yttria (Y_2O_3), aluminium oxynitride (AlON), cubic zirconia (ZrO_2), Mg-Al spinel ($MgAl_2O_4$). The application area is as diverse as the material processing required for the fabrication of the above mentioned ceramics. Alumina finds application as an arc discharge tube for containing the sodium vapour plasma which is corrosive in nature and the transparency of the alumina tube enables the light to pass through the tube and illuminate the streets. Zinc sulphide and aluminium oxynitride are successfully used as window material for Infra-Red sensor used in anti-tank missiles. Zirconia is used as American diamond in jewellery and as dental ceramics which gives an aesthetic value while the dental treatment is still in progress [4].

The first ever transparent ceramic was fabricated by Robert L. Coble in General Electric (GE) who sintered aluminium oxide (*LucAlox)* close to theoretical density by doping it with certain percentage of magnesia by restricting exaggerated grain growth (EGG) [5]. The first transparent ceramic for laser gain media was also made by GE, transparent Nano-yttria was made and named as *Yttralox* [6].

Solid state lasers have the advantage of high repetition rate and high power (>100kW) [7]. The application areas include industry, scientific research and military defence sectors. The focus of solid state laser gain material has completely shifted towards Neodymium doped

Yttrium Aluminium Garnet (Nd: YAG) host material which has required properties for a laser host material. The criteria for a material to be used as laser host are:

- High thermal conductivity in order to quickly remove the heat generated during laser operation.
- Low inclusion or impurity concentration in order to reduce any unwanted absorption of light.
- Optically isotropic crystallographic structures (i.e., cubic crystals), which minimizes scattering due to birefringence.

Particularly in polycrystalline systems, grain sizes should be minimized in order to maximize thermal shock resistance.

The principle on which transparent ceramics act as laser host material is the population inversion within the active ions (Nd) present in the host (YAG) ceramics. Figure 1.2 shows the working of laser.

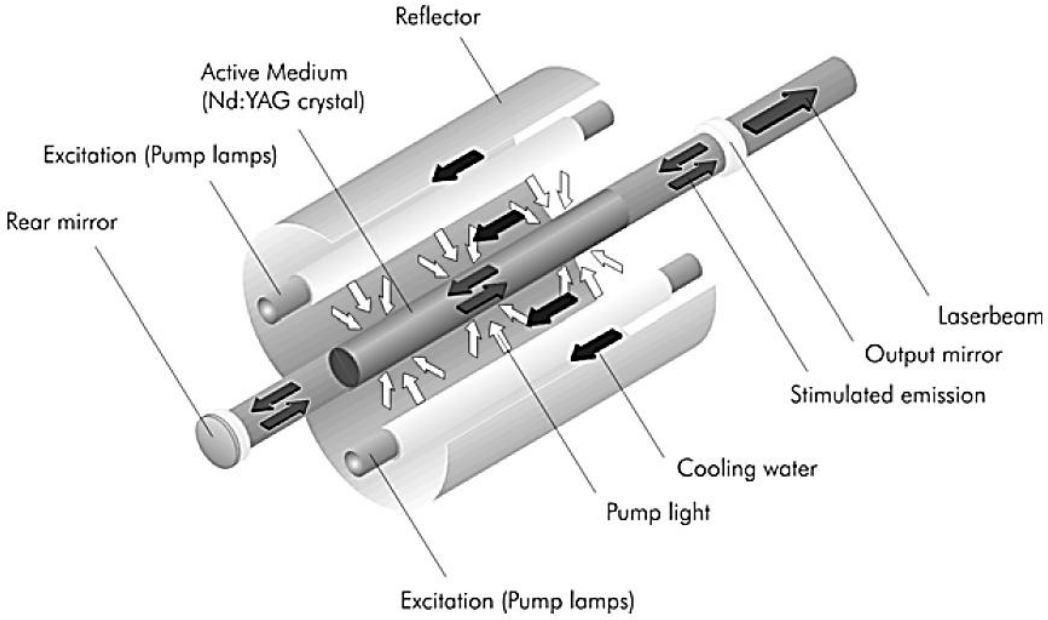

Figure 1.2 Structure of lamp pumped rod laser.

The assembly consist of pump lamp (generally xenon flash light), active lasing medium (Nd:YAG in this case), a rear mirror which is 100 % reflecting, an output mirror which is 95 % reflecting. The pump lamps irradiated the active medium with photons having a wavelength of 540 nm. The energy of these photons pumps Nd^{3+} ions to the highest energy state of the four levels for a certain period of time after which the atom downs to a metastable state by a non-radiative transition followed by a radiative transition to lower laser state by emitting energy in the form of laser, which is having a wavelength of 1064 nm considering Nd: YAG as the lasing medium. The following figure shows a schematic of lasing action.

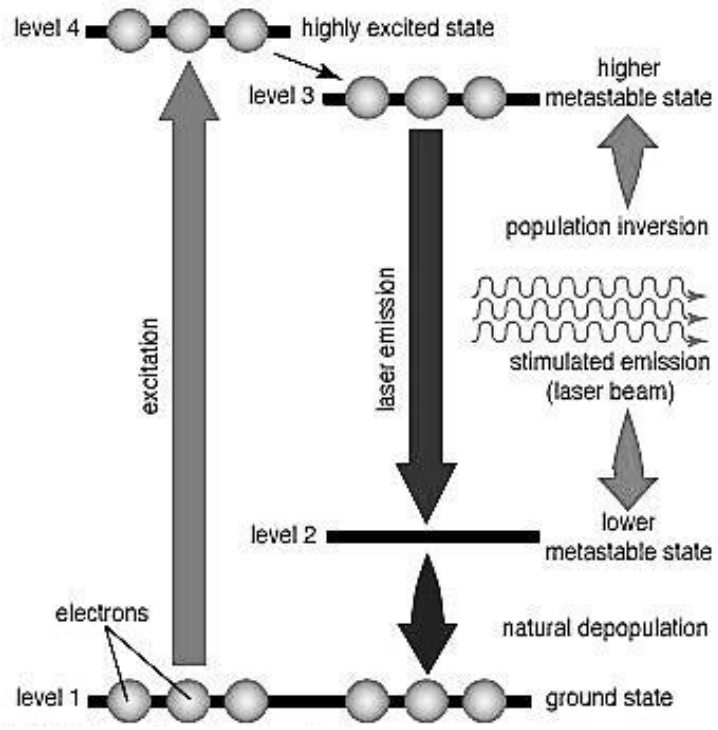

Figure 1.3 A four energy level of solid state laser.

Transparent polycrystalline ceramics have superior properties as compared to the glass ceramic and single crystal counterparts. The production of single crystal counterpart is very energy intensive and expensive process whereas fabricating polycrystalline ceramics need proper ceramic processing and less energy consuming as well as time consuming process.

The following table gives a comparison among glass, single crystal and polycrystalline transparent ceramics.

Attributes	**Glass**	**Single Crystal**	**Polycrystalline transparent ceramics**
Process	Inexpensive Excellent shape formation	Very expensive Simple shapes	Medium costs Complex shaping
Transparency	Very high	Very high	Good Isotropic(macroscopic scale)
Strength/ Hardness	Poor	Good	Frequently better than single crystals
Chemical and Thermal stability	limited	Very high	Good

Table 1.1: Transparent ceramics – Attribute a comparison.

The single crystals are prepared by Czozhralski process, although single crystals can be produced in large simple shapes, they have the disadvantage of a time consuming process for the growth of the crystal, in addition single crystals experience the segregation of the active lasing ion such as Nd^{3+} in case of YAG ceramics [8]. Homogeneous doping in case of single crystals is very difficult, whereas it is possible to dope with up to 9 at. % in case of polycrystalline ceramics. Moreover, intricate shapes can also be made by different green forming such as dry pressing, tape casting, slip casting, gel casting etc.

Yttrium aluminium garnet is cubic crystal with a garnet structure which contains eight formulas per unit cell. The garnet structure can be represented as $\{C_3\}[A_2](D_3)O_{12}$ where C,

A, D represents the do-decahedral, octahedral and tetrahedral sites. The crystal structure [9] can be shown in the following figure:

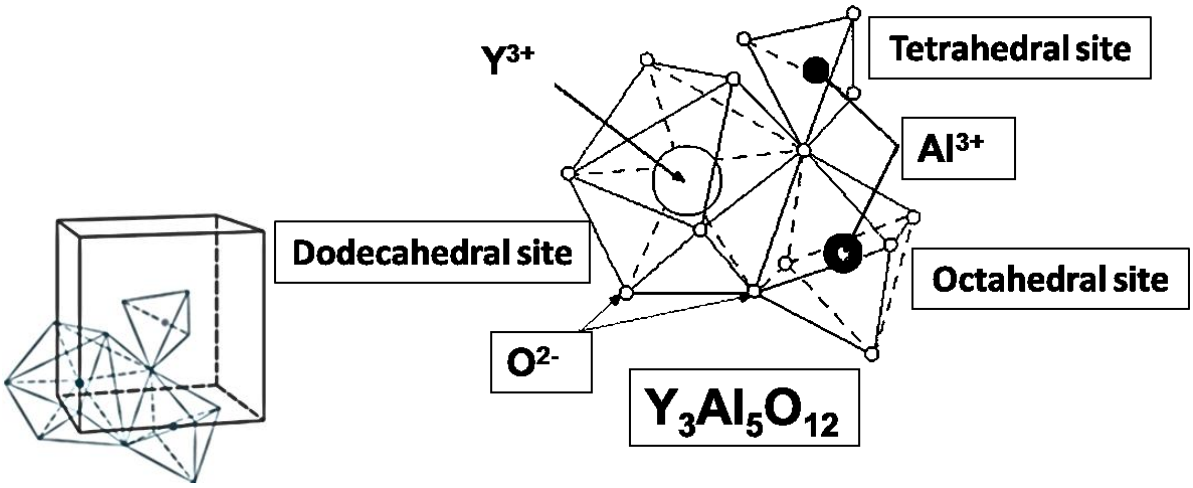

Figure 1.4 Crystal structure of YAG.

YAG is a compound with a cationic ratio of Y:Al in 3:5, hence a slight deviation from the stoichiometry results as secondary phases such as yttrium aluminium monoclinic (YAM – $Y_4Al_2O_9$), and yttrium aluminium perovskite (YAP – $YAlO_3$). The following phase diagram [10] shows the phase field of different intermediate compounds.

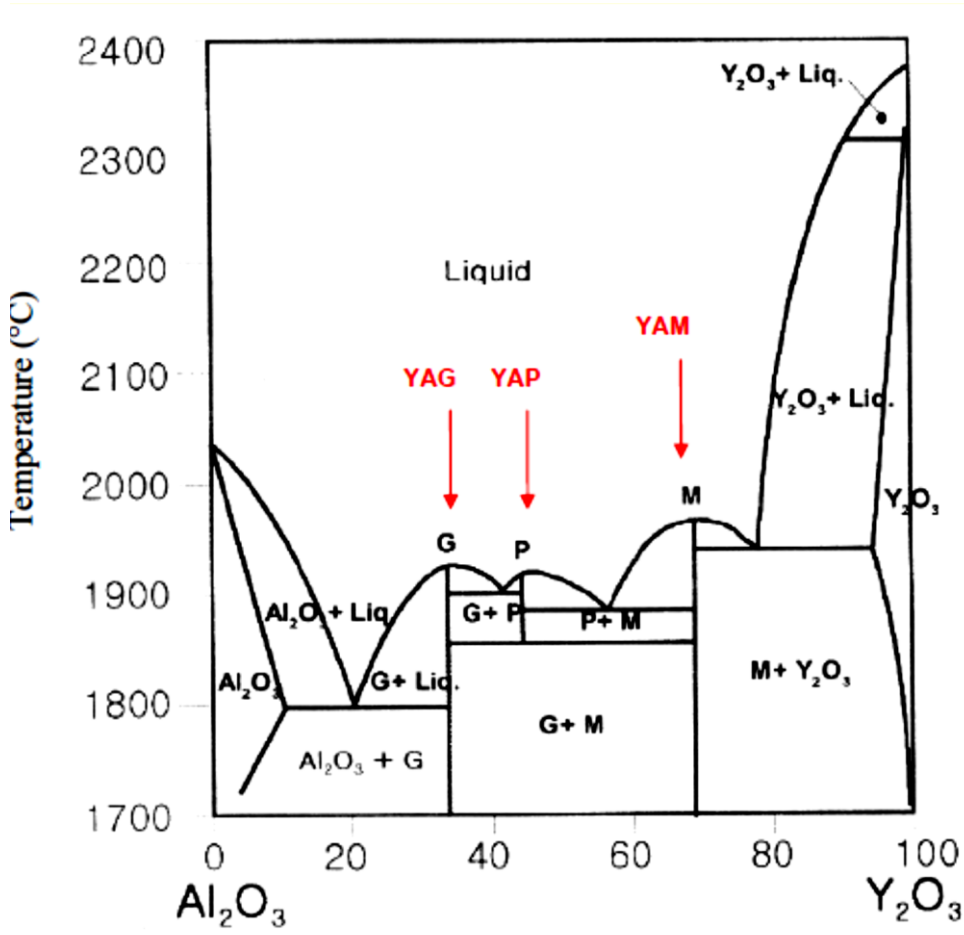

Figure 1.5 Phase diagram of yttria and alumina.

Transparent YAG ceramics are prepared commercially and on lab scale by different methods such as:

- Cold Isostatic Pressing (CIP) of green compacts which are previously consolidated by uniaxial pressing, followed by vacuum sintering at above 1600 ^{o}C.
- Slip casting of YAG ceramic slurry, followed by vacuum sintering in a tungsten mesh furnace.
- Spark plasma sintering of Nano metric YAG particles with a specific uniaxial loading rate and sintering regime.
- Pressure assisted sintering in hot press where simultaneous application of pressure and high temperature helps in achieving density close to theoretical value.

- Pre-sintering of consolidated green body followed by Hot Isostatic Pressing (HIP) which involves application of hydrodynamic pressure and high temperature simultaneously.

The raw material for YAG ceramics can either be stoichiometric mixture of Y_2O_3, Al_2O_3 and Nd_2O_3 powders or Nano-metric YAG particles synthesised by any chemical precipitation route, may it be co-precipitation, sol-gel, hydrothermal or combustion synthesis. In this work, we mainly focus on the synthesis of Nano YAG particles by co-precipitation route. Mixing of oxide and reactive sintering yields pure phase material but the problem lies in the fact that direct conversion of YAG phase does not take place, rather follows formation of intermediate phases like $Y_4Al_2O_9$ (YAM) and $YAlO_3$ (YAP). The wet chemical route gives an advantage of nano size particles as well as a pure phase of YAG at low calcination temperature.

Sintering of YAG ceramics is difficult because of high melting point (1970 ^{o} C) and due to the sluggish diffusion of yttrium ions which may be attributed to the larger size of the same. Hence, special sintering techniques are adapted to achieve transparency of sinter YAG ceramics. Vacuum sintering is widely used technique for YAG ceramics; in addition hot-isostatic pressing, spark plasma sintering and other exotic processing techniques are also successfully used for fabricating transparent YAG ceramics.

The principle involved in vacuum sintering is that sintering is carried out in reduced pressure thereby increasing the pore mobility beyond the grain boundary mobility, further due to reduced pressure the gaseous impurities are excluded from the ceramic compact which includes air or any gases resulting from the decomposition of organic matter.

Scope of the present:

- Synthesis of pure phase of yttrium aluminium garnet ceramic powders by co-precipitation of corresponding metal nitrates against ammonium bicarbonate solution. Standardisation of the above mentioned method for obtaining nano-powders optimised for transparency in ceramics and reproducibility of the same.
- Designing an experiment by modifying the parameters of the above mentioned co-precipitation reaction to obtain Nano-particles by arresting the nuclei in the nascent form and restricting the growth of the same.
- Characterisation of the ceramic powders synthesised thereof for investigating the particle size, particle morphology and surface area, phase evolution with temperature and decomposition behaviour of the precipitates with temperature.
- Investigating the effect of calcination temperature on the atmospheric sintering behaviour of the compacted YAG ceramics.
- Elucidation of the effect of SiO_2 doping in the sintering behaviour of YAG ceramics.
- Spark plasma sintering of ceramic powder selected on the basis of pressure-less atmospheric sintered density obtained after calcination at a particular temperature.
- Evaluation of optical properties of spark plasma sintered compacts

Chapter 2

Literature review

Chapter 2

Literature review

The literature has been studied by categorising the advent of ceramic laser gain media, powder synthesis, consolidation and sintering into sub-sections. Each sub-section will give a brief idea of the processing as well as the modifications in the conventional processing routes.

Evolution of ceramic laser gain media

Robert Coble [11] of General Electric Corporation was the first ceramist to introduce translucent ceramics to the world. An equiaxed microstructure with a grain size of around 30 microns was achieved by doping 500 ppm of magnesia in a sub-micron grade alumina; the sintering was done in a hydrogen atmosphere furnace at a temperature of 1700 ^{o} C. As the molecular size of hydrogen is small due to which the diffusivity is higher than that of air (nitrogen and oxygen) and hence it was possible to remove all the residual porosity rendering the ceramic translucent for use in metal halide lamp and high pressure sodium vapour lamps.

Grescovich [12] was the first to demonstrate the possibility of oxide ceramic laser by fabricating Nd:ThO_2-Y_2O_3 which was successfully implemented for pulsed laser oscillation. After the invention of *Lucalox* General Electric Corporation invented *Yttralox*, which marked the beginning of ceramic-laser technology. Recently the laser power output using transparent polycrystalline YAG has gone above 100 kW. The following figure shows the progressive increase in the laser power output in the last decade.

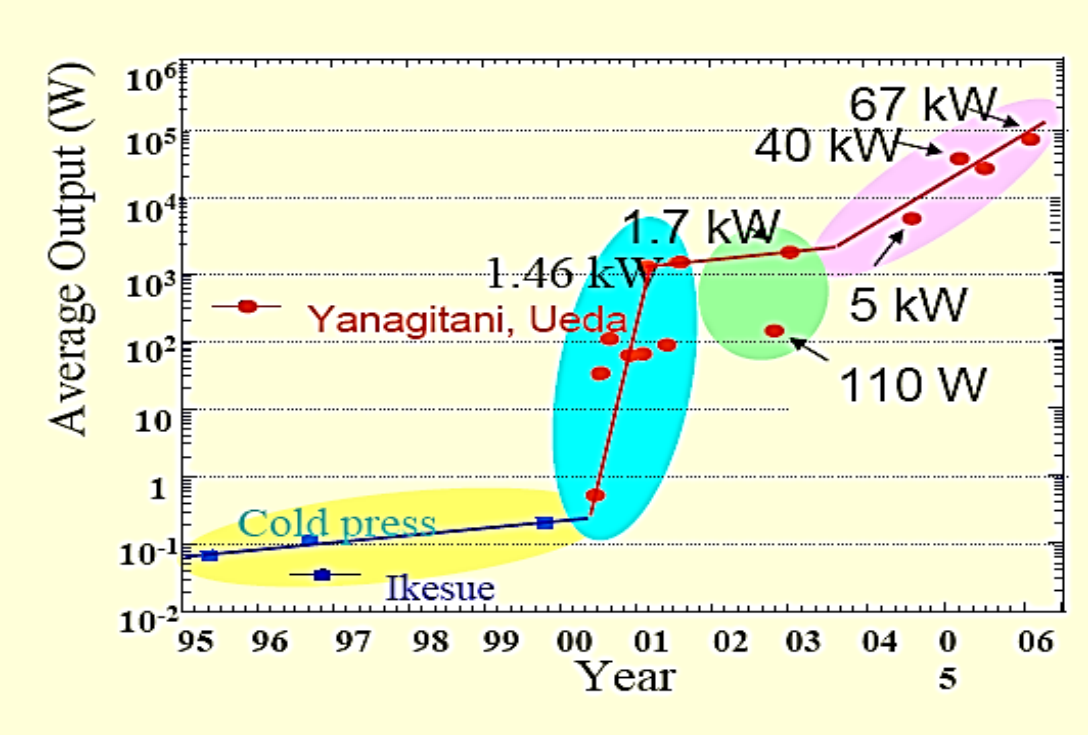

Figure 2.1 Progress of output power over a period one decade.

After 30 years the work of ceramic laser gain media was taken up by Ikesue et.al.[13] , this research group successfully fabricated transparent YAG ceramics by dry pressing of powder followed by vacuum sintering. Recently the work is continued by Messing et al. [14], the method adopted by this research group was tape casting of composite ceramic structure followed by HIPing.

Powder synthesis:

Yttrium aluminum garnet is a stoichiometric ceramic oxide with a cationic ratio of 3:5 for Y: Al. Stoichiometry is very important in case of transparent ceramics because non-stoichiometry leads to secondary phases that can restrict the transparency even when present in minute amount. Moreover the particle size has also a role to play for achieving transparency, as smaller the particle, higher is the specific surface area and higher is the driving force for densification.

Synthesis of YAG is primarily done by two techniques namely solid state process and wet chemical process, where wet chemical process is again divided into sub sections which may include sol-gel process, co-precipitation, combustion synthesis and many more. This thesis mainly focuses on the co-precipitation route of synthesis considering metal nitrate as the precursor for nanoparticle synthesis.

Caroline Marlot et. al. [15] synthesised YAG precursor by using corresponding metal nitrates which was precipitated against ammonium bicarbonate. They performed calcination for one minute at various temperatures, the phases detected at 900 ^{o}C was YAP whereas complete conversion of YAG was possible at 1100 ^{o}C. The complete precipitation reaction was carried out at pH of 7.3, deviating from the pH of 7.3 yielded secondary phases such as YAM and YAP. It was suggested by the research group that the precursors formed by precipitating the metal nitrates against ammonium bicarbonate may have a complex form and that the ligands attached to it might be ammonium, hydroxide, carbonate or bicarbonate. A particle size of around 30 nm was achieved. Broadly a comprehensive study was done by varying the pH, ageing time and calcination temperature.

Xianxue et. al. [16] synthesised YAG by co-precipitation of metal nitrate against tetraethylpentamine. This method is novel because control over pH was not necessary to obtain pure phase material. Moreover a calcination temperature of 900 ^{o}C was enough to convert the precursor into pure YAG phase with a particle size of around 50 nm.

Yuanhua Sang et. al. [17] studied the chemical evolution of YAG precursor by co-precipitation of yttria and aluminium nitrate dissolved in nitric acid and precipitated against ammonium bicarbonate. The precipitates were collected at different points of titration. The pH of the same was measured as a record for the pH regime that the reaction followed. It was observed that a pH greater than 8.0 facilitated the formation of second phases such as YAP or

yttria. A higher pH facilitated re-dissolution of Al^{3+} cation hence disturbing the Y/Al ratio which is actually required for the synthesis of pure YAG. Synthesis of pure YAG was possible at low pH with bi-carbonate precursors only rather than hydroxide precursors. Although the formation of YAG was detected by an exothermic peak in DTA curve but a temperature of 1300 ^{o}C for 3 hours was necessary for complete conversion of YAG. It was realised that lower the aging time, higher was the peak sharpening of YAG and higher was the crystalline nature.

Jiang Li et al. [18] followed a co-precipitation route to synthesise YAG nanoparticle and subsequently sinter it to transparency. In the work done by this group it was observed that the concentration of ammonium bicarbonate solution affected the ultimate composition of the precipitates. Higher concentrations resulted in normal carbonate precursors whereas lower concentration facilitated the formation of a complex precursor having both hydroxide and carbonate groups attached to it. Heat treating the precursor at 800 ^{o} C resulted in the formation of cubic yttria and amorphous alumina. A calcination temperature of 1200 ^{o}C for 3 hours was necessary for obtaining pure YAG phase with a primary crystallite size of 120 nm.

Shaokang Yang et al. [19] modified the process of co-precipitation by citric acid treatment. Use of citric acid enables formation of YAG at 900 ^{o}C in addition to loosely agglomerated powder. The degree of agglomeration was confirmed by TEM analysis. There had been a direct conversion of YAG phase rather than forming intermediate phases such as YAM and YAP. The reason for the reduction in agglomeration is the association of cations with citric acid rather than water molecules.

Vrolijk et al. [20] used sulphate of aluminium and yttrium by refluxing Al metal yttria in sulphuric acid. The precipitant used was sodium hydroxide and the precipitation process was carried out at a pH of 9.0. It was realised that the best dispersion medium was iso-

propanol/ammonia mixture to obtain fine YAG precursor. The precipitant used was ammonia water when precursors were chloride solution.

Zheng et al. [21] synthesised YAG particles with a spherical morphology and a particle size of 100 nm to 500 nm. The reaction medium was supercritical water where respective metal nitrate along with ammonium bicarbonate was used as starting a material followed by heating at 450 ^{o}C under high pressure for 4-6 hours in an autoclave. It was found that the particle size could be controlled by controlling the reaction time in supercritical water. This method does not introduce any organic impurities due to which the ceramic powder can be used successfully for the manufacture of transparent ceramics.

Min Zeng et al. [22] studied the effect of precipitant on the nature of the precipitates obtained. A comparison has been made by using ammonium bicarbonate and ammonium carbonate as the precipitants. It has been observed that the precursors obtained by ammonium carbonate route had secondary phases due to higher pH of the reaction mixture, thereby forming yttria as one of the phases. Thermal analysis suggests that an intermediate YAP phase forms before the formation of YAG. Loosely agglomerated powder was only obtained in case of ammonium bicarbonate as the precipitant. The powders obtained had excellent dispersing and sinterability.

Lian Wang et al. [23] discussed on the effect of ammonium bicarbonate precipitant. A higher concentration resulted in coarse precipitates due to agglomeration because of reduced inter-particle distance whereas low concentration of precipitates enables the formation of agglomerate free powder. Higher concentration of precipitant even resulted in the increase in the calcination temperature to obtain a pure phase YAG, whereas lower concentration provides higher homogeneity thereby reducing the calcination temperature.

Rabinovitch et al. [24] worked on the synthesis of nanometric neodymium doped YAG by freeze drying the precipitates for obtaining agglomerate free particles for transparent ceramic application. The starting materials were aluminium lactate and yttrium acetate, which was boiled with acetic acid and sprayed in a liquid nitrogen bath under vacuum followed by heat treating at different temperatures. Pure phase was obtained at 1200 ^{o}C.

Formation of YAG by proper blending of corresponding solid oxides followed by heat treatment takes place in a series of reaction. The reaction can be represented as:

$$2Y_2O_3 + Al_2O_3 \rightarrow \text{YAM (900 – 1100 ºC)}$$

$$\text{YAM} + Al_2O_3 \rightarrow \text{4YAP (1100 – 1250 ºC)}$$

$$3\text{YAP} + Al_2O_3 \rightarrow \text{YAG (1400 – 1600 ºC)}$$

The synthesis of YAG by solid state route is the easiest because the problem of stoichiometry does not arise. The reaction basically proceeds by the diffusion of Al^{3+} into yttria lattice because of the smaller size of aluminium ion. As the reaction proceeds the Y/Al ratio decreases suggesting the diffusion of Al into yttria.

Consolidation

The fabrication of transparent ceramics is very tricky and it needs defect free processing of green bodies. Achieving a density close to theoretical is only possible if the green body is manufactured by great care with proper ceramic processing. The different consolidation technique adopted are uniaxial dry pressing, cold isostatic pressing (CIP), slip casting, gel casting (thermal and nonthermal) and tape casting. A considerable amount of work is done adopting uniaxial dry pressing and cold isostatic pressing. CIP has an advantage of uniform density because of hydrodynamic pressure whereas uniaxial pressing results in a density gradient when the sample thickness increases. It is also observed in many published research

that uniaxial pressing is done for shaping followed by CIP for attaining a better green density. Slip casting is another technique used for ceramic body fabrication; this method is considered to be the best for the preparation of large shaped transparent ceramics because of homogeneous density and product volume. Slip casting is done by dispersing the ceramic powder in water by adding certain dispersant and maintaining the pH to obtain the isoelectric point of the specific ceramic powder to avoid flocculation. The solid loading of the slurry is also optimised to obtain a higher green density. The slurry is then cast into porous plaster of paris mould which sucks away the water content of the slurry and there by forming a ceramic body which can be considered as big hard agglomerate. Gel casting is a technique in which the ceramic powder is mixed with a monomer and homogenised in a slurry form, at a later stage cross linking polymer, catalyst and initiator is added to commence the polymerisation reaction after which a ceramic body is formed which has a high flexural strength as well as machinability which facilitates us to cut and shape it into desired specification. Tape casting of ceramic slurry by using a doctor blade assembly is done for making composite ceramic body by stacking tapes with different dopant concentrations. Messing et al. [25] successfully adopted the technique of tape casting to fabricate transparent YAG ceramics.

There are certain consolidation techniques, which combines both the application of pressure and temperature simultaneously such as hot pressing, hot isostatic pressing (HIP), spark plasma sintering (SPS), field assisted sintering, etc.

Sintering

Sintering is a phenomenon of densification along with grain growth. The main sintering practices for fabricating transparent ceramics are hot pressing, hot isostatic pressing (HIP), spark plasma sintering (SPS), vacuum sintering, microwave sintering. Among the mentioned sintering practices HIP and vacuum sintering is successfully used for transparency in YAG ceramics. SPS processing for attaining transparency in YAG is in a stage of development.

Greskovich et al. [6] were the first to sinter an oxide ceramic laser gain material to transparency by sintering the pre-sintered compacts in hydrogen atmosphere. The hydrogen molecule has a higher diffusivity and hence elimination of all residual porosity is possible.

Ikesue et al. [13] was able to achieve transparency in YAG by dry pressing spray dried powder followed by vacuum sintering in a refractory metal furnace. The average grain size of the transparent YAG ceramic was 20-30 microns. Ikesue and Aung [7] prepared the polycrystalline transparent Nd:YAG from Y_2O_3(60nm), Al_2O_3(300nm), Nd_2O_3(500nm) through vacuum sintering and compared the continuous wave (CW) laser performance of a commercial high quality 1 at% Nd:YAG single crystal with that of pore-free 1.0, 2.4 and 3.6 at.% Nd:YAG polycrystalline ceramics pumped with a Ti:Sapphire laser (808 nm). The threshold and the slope efficiency of polycrystalline Nd:YAG ceramics generally depend on the Nd concentration because fluorescence lifetime decreases with increase in Nd concentration. However, they achieved very high laser conversion efficiency in each of the ceramic samples, which was attributed to their pore-free condition. Although optical resonators were not optimized in this oscillation, the slope efficiency (Z) of the polycrystalline ceramics was as high as 65%, and this value is almost equivalent to that of a single crystal.

In another attempt, Lee et al [26], have fabricated transparent polycrystalline Nd:YAG ceramics by solid-state reactive sintering from a mixture of commercial α-Al_2O_3 (0.1–0.3 μm), Y_2O_3 (2 – 4 μm) and Nd_2O_3 (1–2 μm) oxide powders. The powders were mixed in methanol and doped with 0.5 wt% tetraethoxysilane (TEOS), dried, and pressed. Pressed samples were sintered from 1700^o to 1850^o C in vacuum. Transparent fully dense samples with average grain sizes of ~50 μm were obtained at a sintering temperature of 1800^oC for all Nd_2O_3 levels studied (0, 1, 3, and 5 at%). The in-line transmittance was >80% in the 350–900 nm range regardless of the Nd concentration. The best of 84% transmittance was achieved 1 at% Nd:YAG ceramics (2 mm thick), which is equivalent to 0.9 at.% Nd:YAG single crystals grown by the Czochralski method. However, the thermo-mechanical properties of these samples with such large grain size may not be suitable for high energy applications and hence a smaller grain size needs to be attempted.

Konoshima Chemical Co. Ltd, Japan is preparing this quality of Nd:YAG ceramics from nanopowders as obtained through co-precipitation technique followed by vacuum sintering. On the other hand, Raytheon, USA used hot isostatic pressing of doped nanopowders to achieve transparency [27]. There are others, who have used spark plasma sintering technique to develop transparency in YAG ceramics. Each of these three processing routes have their advantages as well as limitations: Spark Plasma Sintering (SPS) is normally suitable for smaller disk (Ø ~10mm, thickness ~2mm) only, Cold Isostatic Pressing/Slip casting followed by Vacuum Sintering for relatively larger rod (Ø 0.5 – 10 mm, Length ~ 1 - 100mm) and Dry Pressing/Tape casting followed by hot isostatic pressing for plate like shapes (45 x 45 x 3mm).

Fabrication Techniques	Particle Size (nm)	Temperature (^{o}C)	Pressure	Time	Grain Size (μm)
SPS [28]	34±17	1400	100 MPa	3Min	~1
Vacuum Sintering [29]	~40	1800	10^{-6} torr	4hr	~2
HIP [30]	~100	1650	200MPa	6hr	~5

Table 2.1 Different Techniques of Preparing Transparent Polycrystalline YAG.

National status

There have been a relatively small number of attempts by the Indian researches for the study/ development of this material. The institutions like *BARC, CGCRI, ARCI, RRCAT, LASTECH* etc. have attempted in a limited manner to investigate various techniques of powder synthesis followed by sintering under normal atmospheric condition and for obvious reasons have gained limited success [31-34]. In brief, Ramanathan et. al [31] synthesized YAG micron powders through homogeneous co-precipitation reaction of aqueous aluminium nitrate-yttrium nitrate-urea in presence of ammonium sulphate at 95 ^{o} C. The precipitate was filtered, washed, oven dried at 85 ^{o}C, ground to break down the agglomerates and subsequently calcined at 1300^{o} C to prepare 2.2 μ m YAG powder. The average 5 μ m sintered grain size of 53% dense green compact was achieved after vacuum sintering at 1700^{o}C for 5h in an electron bombardment furnace, which exhibited 60% transparency in the range of 300 to 1100 nm. However, other sintering technique reveals near to fifty times growth of starting powder size after sintering to achieve equivalent properties of single crystal.

Bhattacharyya et. al [32] prepared the micron size (-300mesh or 50 μ m) YAG powder through wet-chemical route and achieved 93% densification with 2.5wt% silica after CIPed at 250MPa and atmospheric sintering at 1650^{o} C, which was completely opaque due to low temperature atmospheric sintering of hard agglomerated powders. Recently, Singh et. al [33] developed a poly-esterification technique to prepare 3% Nd doped YAG nanopowders. The particle size of hard agglomerate ranges between 50 and 100nm, however, they have not reported preparation of transparent ceramics from such powders. Microwave flash combustion technique has been adapted by Chowdhury et. al [34] to synthesize Nd doped YAG nano-powders, and the particle size was found to vary in the range of 24-70 nm having very little agglomeration. Once again no sintering studies have been carried out to attempt preparation of the transparent ceramics. It may be noted that formation of hard agglomerates, wider particle size distribution and appropriate powder consolidation and sintering conditions (temperature and atmosphere) are the major requirements to obtain transparent polycrystalline ceramics. It is needless to mention that extensive experimentation together with proper understanding of the defect chemistry of the material is essential in order to achieve ultimate objective of preparing the transparent ceramics with the desired optical as well as the thermo-mechanical properties.

Chapter 3

Experimental

Chapter 3

Experimental

Nitrate solution of Al^{3+} was prepared by dissolving Aluminum nitrate in distilled water and maintaining a concentration of 0.15M. Yttrium oxide was added to the nitrate solution with constant stirring and mild heating and addition of few drops of diluted HNO_3. The salt solution was cooled below room temperature and the ammonium bicarbonate solution was also precooled before carrying out the precipitation reaction at a constant pH of 7.3. The overall temperature of the reactants and precipitant was around 10 ^{o}C. Chemical precipitation was performed by the reverse strike method (adding salt solution to ammonium bicarbonate solution. The reaction mixture was aged for about half an hour after which the contents were refrigerated centrifuge at 10 ^{o} C. The precipitates were washed four times to get rid of ammonium nitrate if any. The precipitates were then freeze dried at -53 ^{o} C. Thermal analysis of the precipitates were done upto a temperature of 1200 ^{o} C. FTIR spectroscopy was performed on as-precipitated powder and powders calcined at 900 and 1100 ^{o} C. The precipitates were calcined at 900 and 1100 ^{o} C in a muffle furnace. Phase analysis were done using X-ray diffraction technique. Surface area of the powders calcined at 900 and 1100 ^{o} C were measured by BET. The particel size of the ceramic powder were confirmed by TEM micrographs.The sintering of the powders calcined at 900 ^{o} C were pressure-less sintered at 1650 ^{o} C and spark plasma sintered at 1300 ^{o} C only for maximum density obtained after atmospheric sintering. The sintered samples were polished with varying grades of diamond slurry to obtain a mirror finish followed by thermal etching at 1550 ^{o}C to reveal the grain boundaries. The mcirostructure of the thermally etched samples were revealed in a scanning electron microscope. The polished spark plasma sintered samples were analysed in a UV-VIS

spectrophotometer for obtaining the absorption and transmission percentage. The optimised scheme of nanopowder synthesis is given in the following flow sheet.

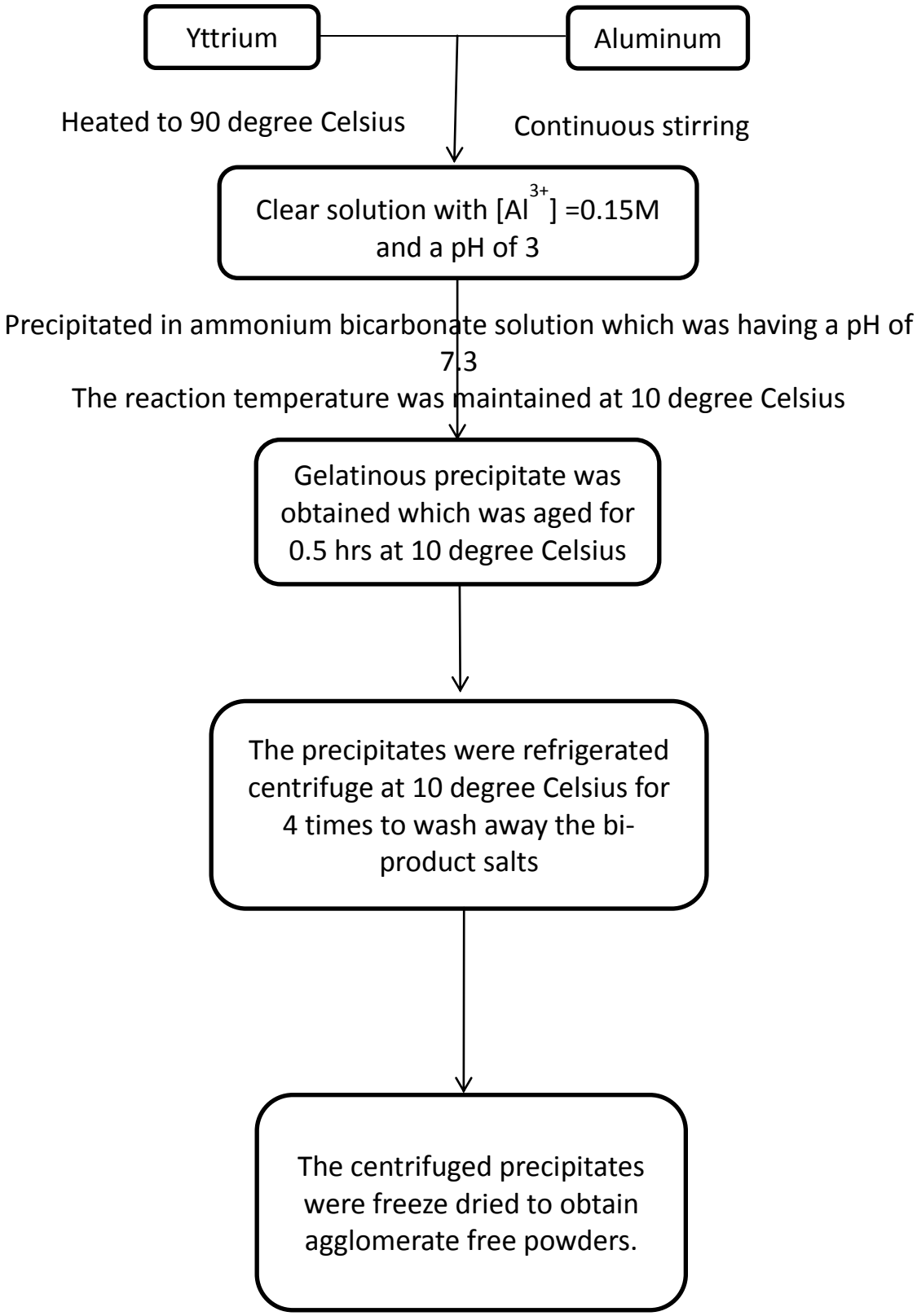

Chapter 4

Characterization of synthesised YAG powders

Chapter 4

Charecterisation of synthesised YAG powders

4.1 Thermal analysis by Differential Scanning Calorimeter (DSC) and thermogravimetry (TG).

The temperature of phase transformation and the decomposition behaviour of the as-precipitated powders were done by DSC-TG (NETZSCH STA 449C, Germany). It uses a couple of thermocouple attached to the sample and reference and this thermocouple is used to measure the heat evolved or absorbed during the heating regime. The thermocouple generates small current or signal due to seebeck effect, the instrument is further calibrated to convert the signal into the heat evolved. An exothermic reaction results in the evolution of heat and is represented by a peak in the plot of temperature vs. heat evolved, similarly for an endothermic reaction a dip occurs in the plot. The samples were heated at a rate of 10 ^{o} C/min upto a temperature of 1200 ^{o} C. The variation in the heat evolved is plotted against the temperature in Figure 4.1.

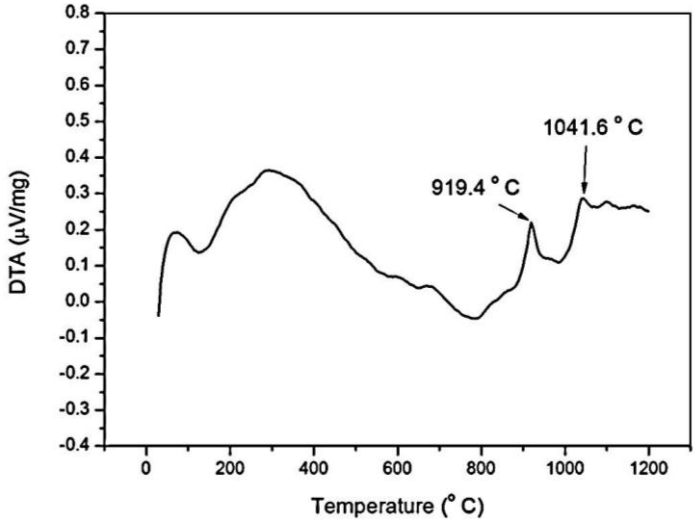

Figure 4.1 DTA of as-precipitated YAG precursor.

The diffused endothermic peaks at around 100 ^{o} C relates to the evaporation of physically absorbed water, the wide peak ranging from 200-400 ^{o} C corresponds to the decomposition of residual ammonium nitrate and chemically absorbed water i.e. breaking of OH bonds. The sharp exothermic peaks at around 920 and 1050 ^{o} C corresponds to the phase formation of YAP and YAG, respectively.

Thermogravimetrc analysis is the measurement of weight change of sample with increase in temperature. It works on a principle of electro-mechanical transducer which directly connected to the TG crucible. During heating the sample might lose or gain weight depending on the nature of the sample. In general decomposition results associated with the reduction of the weight. The powder sample is loaded on a small crucible which is mounted on sensitive mass sensor and is surrounded by heating coils and thermocouple to monitor the temperature. The powder precipitate is heated at rate of 10 ^{o} C/min upto 1200 ^{o} C. Figure 4.2 shows the plot of mass loss vs temperature.

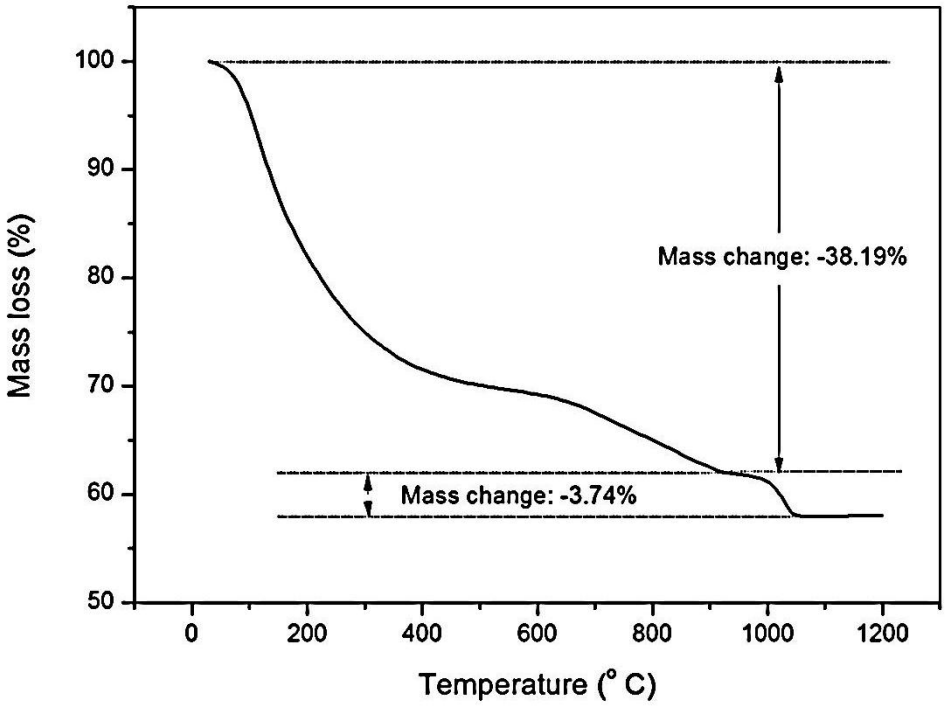

Figure 4.2 TG of as-precipitated YAG precursor.

The plateau in the range of 400-600 ^{o} C refers to the decomposition of hydroxide bonds. Furthermore, a total mass loss of around 40 % suggests that the precipitate is a complex ofhydroxide, nitrate and bicarbonates. The mass loss is complete at around 1050 ^{o}C.

4.2. Phase identification by X-ray Diffraction

Phase analyses of the as received powders were performed by x-ray diffraction (XRD) using Cu Kα radiation in Phillips PANalytical (Model: PW 1830diffractometer, Netherland). The XRD system was equipped with 1-dimensional compound silicon strip detector for high quality diffraction data. The powder samples were loaded on a non-diffracting sample holder placed in the Bragg-Brentano diffractometer setup.

The as recorded XRD profiles were normalized to 100% in each case. The background correction as well as $K\alpha_2$ stripping using Rachinger's method was performed prior to the phase analysis using X'pert High Score program with JCPDS database. Identification of a crystalline phase was based on comparison of the observed d-spacing and relative intensities with those of a reference material pattern compiled in the JCPDS database. The X-ray diffraction pattern for standard YAG sample is shown in Figure 4.3

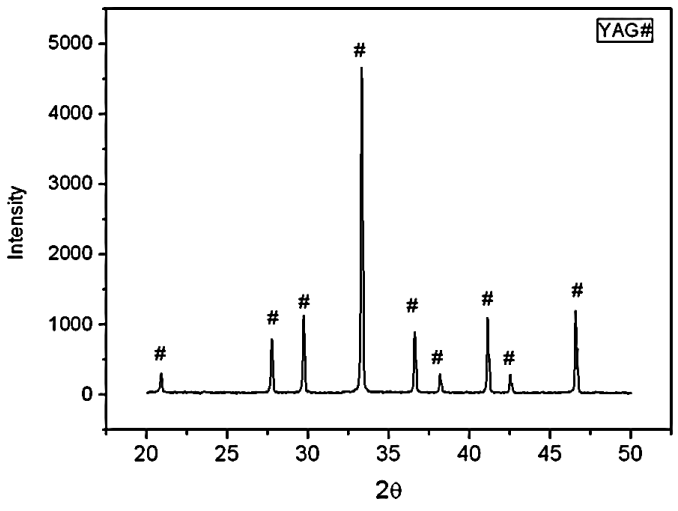

Figure 4.3 Standard intensity pattern for YAG.

XRD measurements were done on as precipitated powder and samples calcined at 900, 1000, and 1100 ^{o} C for varying time of 15, 30 and 60 minutes for each temperature. Figure x shows the X-ray diffraction pattern for samples calcined at 900 ^{o} C.

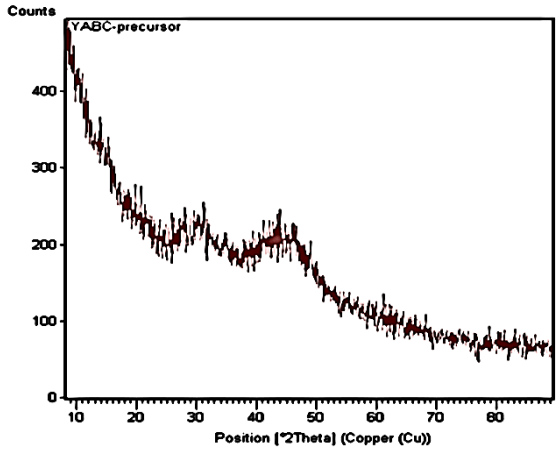

Figure 4.4 XRD pattern of precursor.

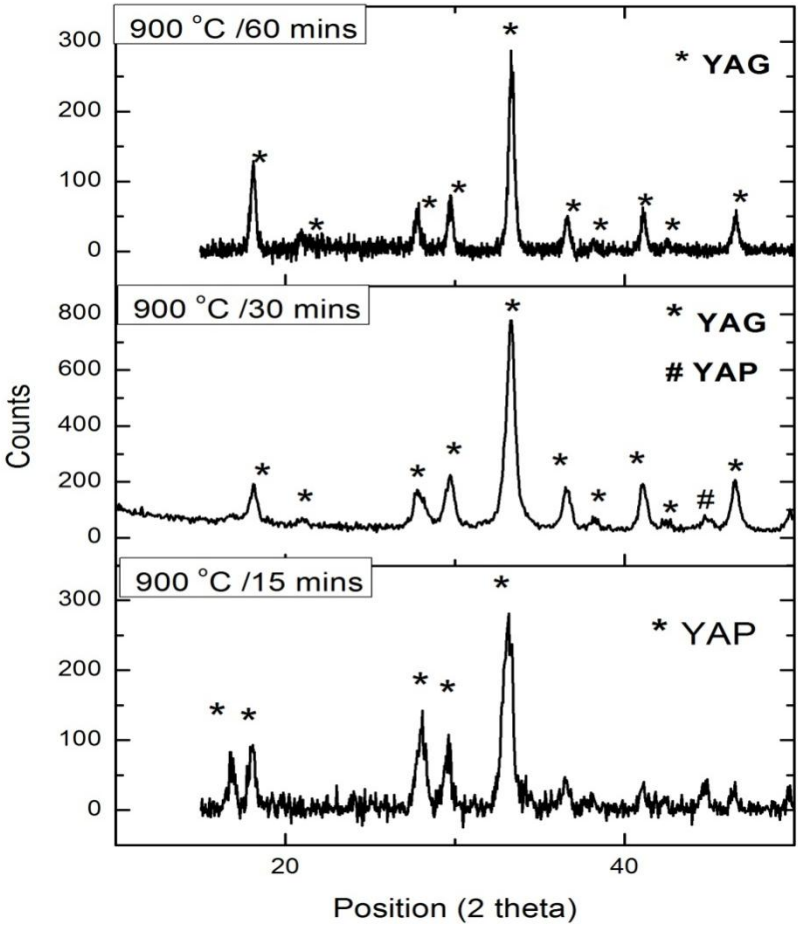

Figure 4.5 Evolution of phase at 900 ^{o} C with varying time.

The diffused peak of uncalcined powder is due to the amorphous nature of the precipitates with expected mixture of bicarbonate and carbonate of Al and Y metal. The XRD pattern revealed that there is a transient phase of YAP exists at a temperature of 900 ^{o}C which when heat treated for longer time converts to pure YAG. The phase change can be realised to be particle size induced transformation or in another way it can be understood that after allowing enough time for Al^{3+} ions to diffuse into yttria lattice.

By heat treating the powders at a temperature of 1000 and 1100 ^{o}C pure phase powder is obtained even at calcination time of as low as 15 minutes. The following figure elucidates the same.

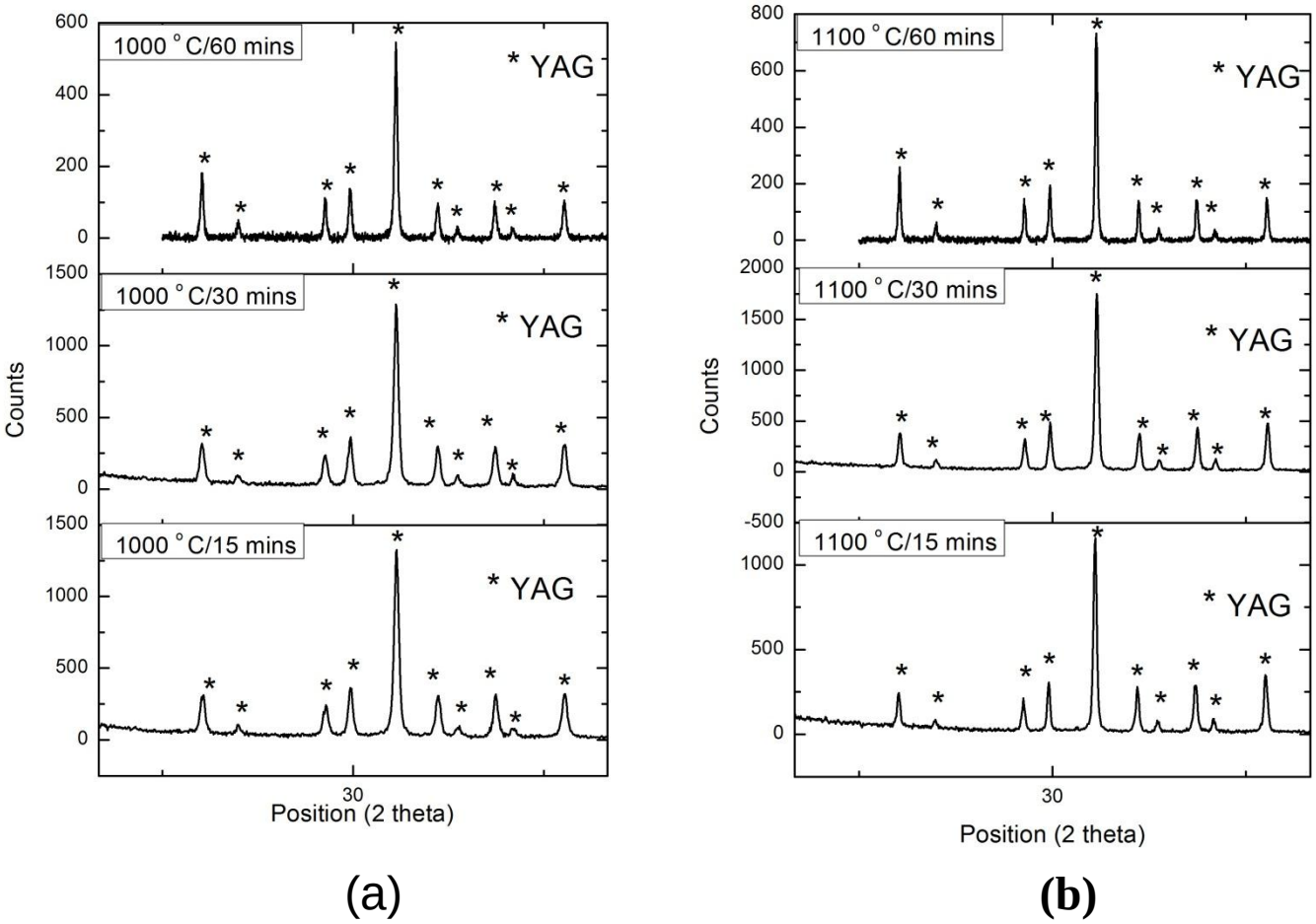

Figure 4.6 Evolution of phase at (a) 1000 ^{o}C (b) 1100 ^{o}C with varying time.

The XRD pattern shows phase purity in each case, the intensity of the peaks seems to increase with temperature indicating the increase in crystallinity of the powders; moreover an increase in temperature decreases the peak broadening suggesting the increase in crystallite size with temperature.

4.3 Zeta potential of powder suspension

Zeta potential measurements of the calcined powder were carried out by determining the electrophoretic mobility and then applying Henry equation. The electrophoresis mobility was measured by measuring the velocity of the particles using Laser Doppler Velocimetry (LDV). The **Henry equation** is :

$$U_E = \frac{2\,\varepsilon\, z\, f(ka)}{3\eta}$$

Where U_E, z, ε, η and $f(ka)$ are electrophoretic mobility, zeta potential, dielectric constant, viscosity and Henry's function.

The most important factor about zeta potential is the pH of the suspension. A pH below 7.0 suggests the presence of H^+ ions which might be adsorbed on the surface of the particles; similarly an alkaline suspension has negative charge which contributes to the electrophoretic mobility thereby affecting the zeta potential ultimately. Zeta potential measurements were done with very dilute YAG (0.1gm YAG powder in 20ml water) suspension with a few drops of Darvan C added as dispersant. The above experiment was repeated by adjusting the pH to the desired value. The following figure shows the variation in zeta potential with the change in pH.

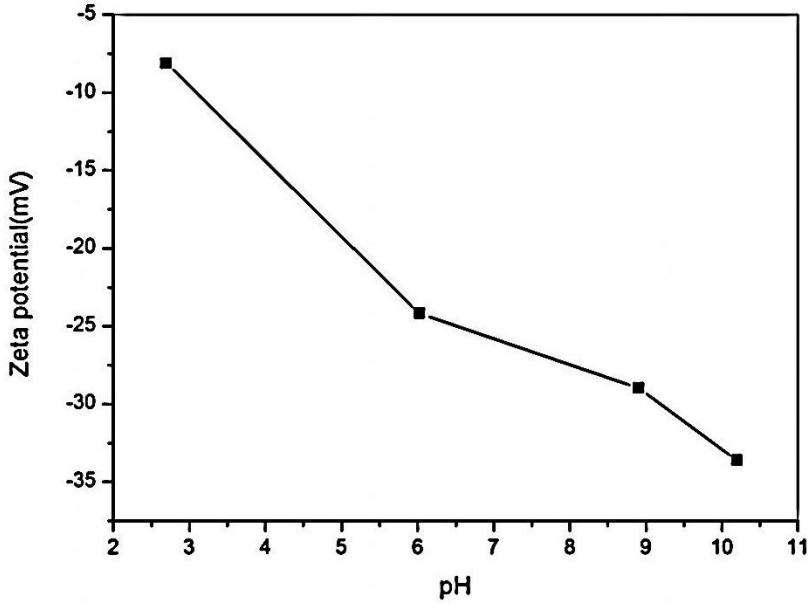

Figure 4.7 Variation in zeta potential with the change in pH.

The above figure suggests that a higher pH is suitable for the dispersion of YAG particles in water and hence for particle size measurement by light scattering method, a high pH is maintained thereof.

4.4 Particle Size Analysis by Dynamic Light Scattering(DLS).

Particle Size Analysis of the as calcined powder was carried out using Photon Correlation Spectroscopic measurements. Photon Correlation Spectroscopy is based on the measurement of the velocity of particles diffusing due to Brownian motion. The random movement of particles in a liquid media due to the inter-particle collision is known as Brownian motion. This motion causes fluctuations of the local concentration of the particles resulting in local in-homogeneities in the refractive index of the material. This in turn leads to Rayleigh scattering spectrum with line width Γ (defined as the half-width at half-maximum), which is proportional to the diffusion coefficient D of the particles (2.1):

$$\Gamma = Dk^2 \qquad (4.1)$$

Where k = $(4\pi n/\lambda)$ sin $(\theta/2)$, n is the refractive index, λ the laser wavelength, and θ the scattering angle. Assuming the particles to be spherical and non-interacting, one can obtain the mean radius 'r' from the Stokes-Einstein equation (2.2).

$$D = \frac{K_B T}{6\pi\eta r} \qquad (4.2)$$

D – Diffusion coefficient, k_B-Boltzmann constant, T - absolute temperature, r – particle radius, and η – Coefficient of viscosity of the medium.

Particle size analysis was carried out by dispersing 0.05 gram of as received powder in 100 ml de-ionized water using dispersant Darvan C i.e., ammonium polyacrylate (R. T. Vanderbilt Co., Inc., Norwalk, CT, USA). Suspensions were ultrasonicated for 30 minutes using Sonicator to ensure the homogeneity and filled into the glass cuvette. The well dispersed suspensions based on zeta measurements were subjected to DLS measurements using Nanosizer (Malvern^{TM}) and particle size distribution curve is shown in Figure 4.8

			Diam. (nm)	% Intensity	Width (nm)
Z-Average (d.nm):	232.6	Peak 1:	295.6	86.4	58.86
PdI:	0.225	Peak 2:	88.50	13.6	10.49
Intercept:	0.945	Peak 3:	0.000	0.0	0.000
Result quality :	Good				

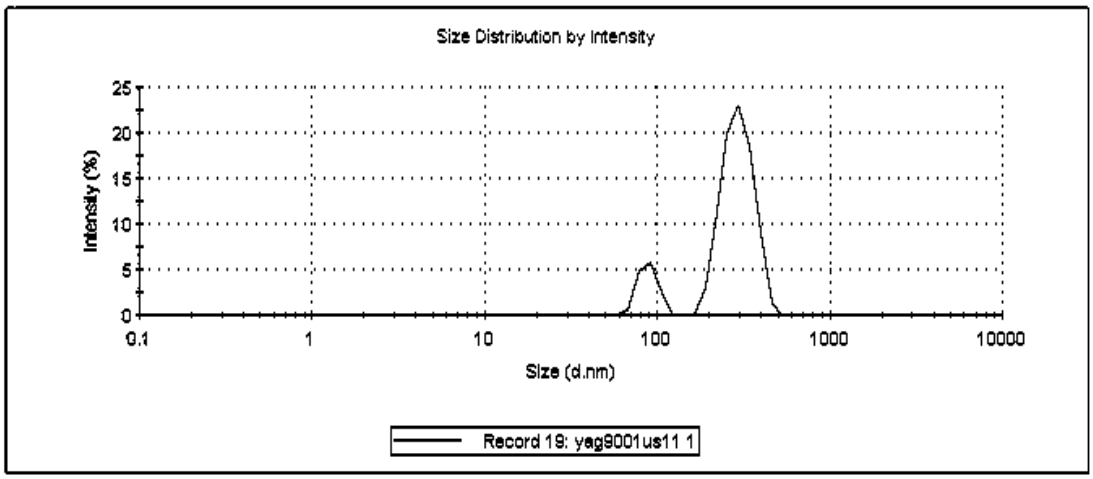

Figure 4.8 Particle size distribution of YAG calcined at 900 ^{o}C for 1 hr.

Particle size analysis exhibits bimodal distribution; near to 50nm and 500nm, respectively. As the expected particle size was below 50 nm and micrographs revealed by TEM suggest a particel size below 50 nm, it was thus infered that due to high surface area the particles tend to agglomerate and the particle size values are actually the size of agglomerates. Moreover the particle size distribution was realised to be bimodal which might help during compaction for attaining high green density.

4.5 Analysis of functional groups by Fourier Transform Infra-red spectroscopy

Infra-red spectroscopy is a way of doing chemical analysis by obtaining a spectrum. The spectrum is obtained by allowing Infra-red waves to pass through the sample and the transmission percentage is plotted against the wavenumber. As a matter of fact each kind of bond has specific bond energy and a specific wavelength is required to excite that bond, hence in a way each bond has its Infra-red signature. The obtained spectrum has peaks and dips which suggests corresponding part of the spectrum being absorbed by the sample. The corresponding absorbed wavenumber is then matched with IR spectroscopy database to know the kind of functional group due to which the peak or dip has appeared.

As-precipitated sample and samples calcined at 900 and 1100 ^{o}C were analysed using FTIR (IR Prestige 21, Shimadzu, Japan). KBr pellets were put into the sample holder and a blank run was done to obtain a background pattern which can later be subtracted from the experimental data. The powders were blended with KBr as KBr is not IR active and is highly ductile. The Figure 4.9 shows the IR spectrum of the analysed samples.

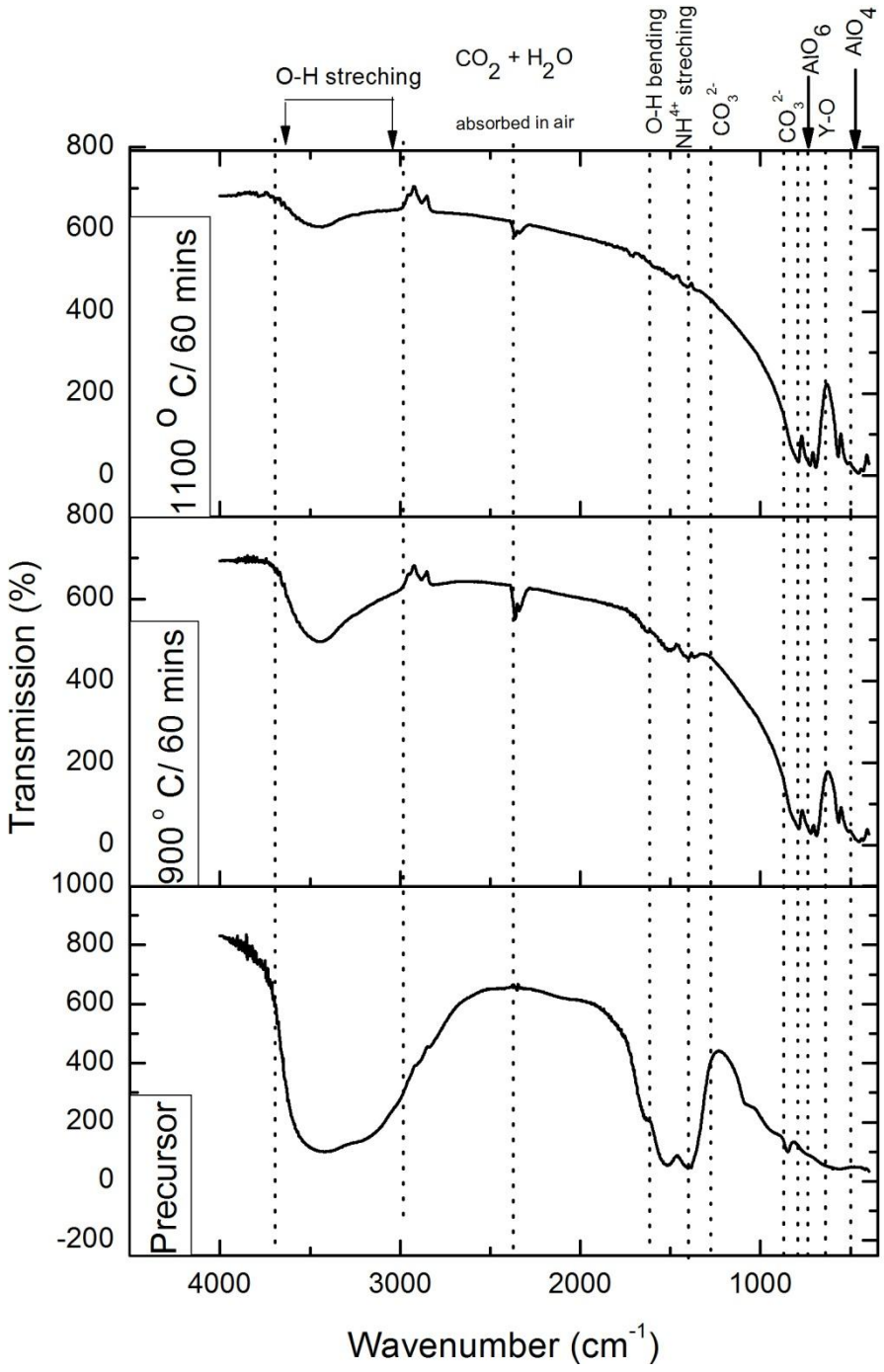

Figure 4.9 FTIR pattern of samples calcined at different temperature.

As the temperature increases the hydroxide bonds break and disappears, however, existence of carbonate ions is still detected even at higher temperature of 900 ^{o} C. At still higher temperatures the peaks of Al-O and Y-O are visible due to formation of respective oxides.

4.6 Surface area measurements by BET

Surface area is measured by physisorption of nitrogen forming a monolayer on the surface according to Langmuir theory. The nitrogen adsorption is done at liquid nitrogen temperature and the degassing is done at 200 ^{o} C for 3 hours. The amount of adsorbed gas recovered is a measure of the specific surface area of the sample. The obtained data is treated according to the adsorption isotherm equation.

$$\frac{1}{\left[V_a\left(\frac{P_0}{P}-1\right)\right]}=\frac{C-1}{V_mC}\times\frac{P}{P_0}+\frac{1}{V_mC}$$

Where

P = partial vapour pressure of adsorbate gas in equilibrium with the surface at 77.4 K (b.p. of liquid nitrogen), in pascals,

P_o = saturated pressure of adsorbate gas, in pascals,

V_a = volume of gas adsorbed at standard temperature and pressure (STP) [273.15 K and atmospheric pressure (1.013×10^5 Pa)], in millilitres,

V_m = volume of gas adsorbed at STP to produce an apparent monolayer on the sample surface, in millilitres,

C = Dimension-less constant which is related to the enthalpy of adsorption of the adsorbed gas on the powder sample.

Then the BET value:

$$\frac{1}{V_a\left(\frac{P_0}{P}-1\right)}$$

is plotted against P/P_o according to equation as shown in Figure 4.10.

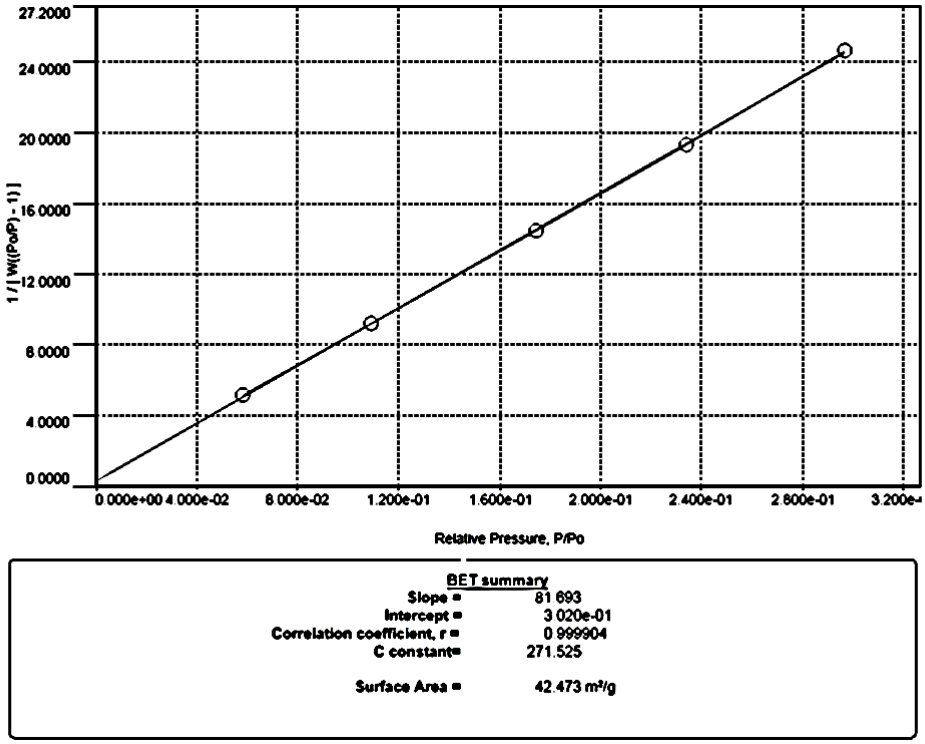

Figure 4.10 Adsorption isotherm of YAG calcined at 900 ^{o}C for 1 hr.

The surface area is then calculated according to the equation:

$$S = \frac{V_m N_a}{m \times 22400}$$

N	=	Avogadro constant (6.022×10^{23} mol^{-1}),
a	=	effective cross-sectional area of one adsorbate molecule, in square

		metres (0.162 nm^2 for nitrogen and 0.195 nm^2 for krypton),
m	=	mass of test powder, in grams,
22400	=	volume occupied by 1 mole of the adsorbate gas at STP allowing for minor departures from the ideal, in millilitres.

The surface area were measured with samples calcined at 900, 1000, 1100 ^{o} C with Quantachrome Nova Autosorb (Quantachrome instruments, USA). The following figure shows the variation is surface area with increasing calcination temperature.

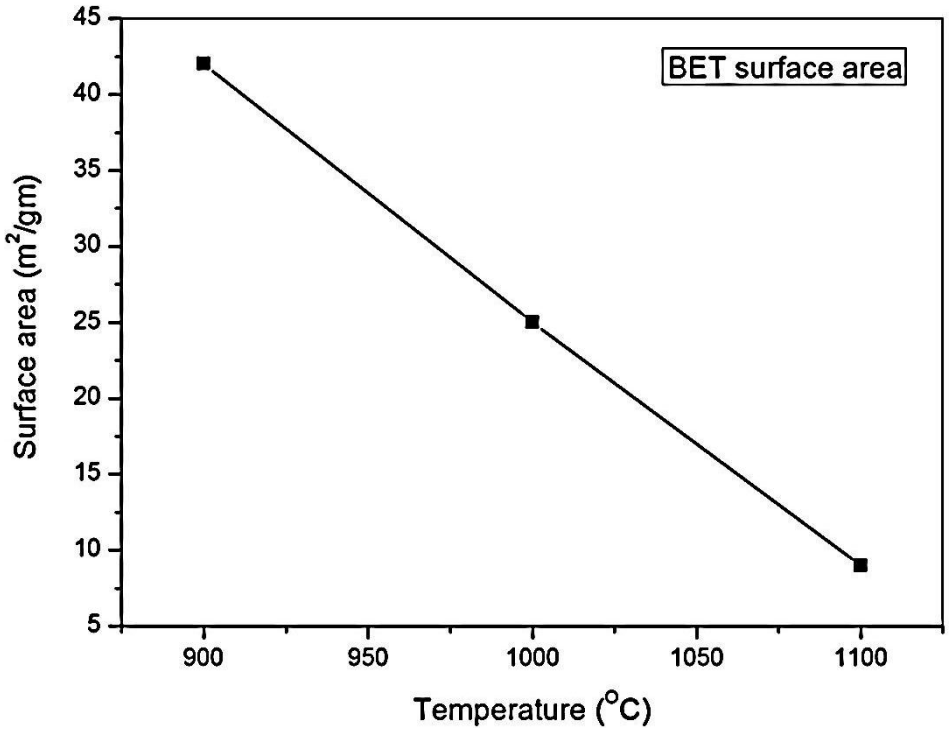

Figure 4.11 Variation in surface area with increasing temperature.

The highest surface area obtained for the powder calcined at 900^{o}C is around 42m^2/gm, which is one of the highest values reported in literature. The decrease in surface area is due to increase in particle size with increasing temperature. The system tries to reduce its energy

by reducing the surface energy which depends on the total surface area. This study supports the selection of calcination temperature for as-precipitated precursors.

4.8 Particle size and morphology analysis by Transmission Electron Microscopy (TEM)

TEM uses an electron beam accelerated by a potential difference of as high as 120 KV. The electron beams is transmitted through the sample and is detected by an electron sensitive screen. The electron interacting with sample scatters, the scattering process may be elastic or inelastic. Elastic scattering gives rise to diffraction patterns whereas inelastic scattering along the grain boundaries, inclusion, dislocations causes a complex phenomenon to occur.

The samples calcined at 900 ^{o}C and 1100 ^{o}C for 60 minutes were analysed in TEM (FEI, Tecnia G2 20). The following micrograph shows the difference between samples calcined at 900 and 1100 ^{o}C.

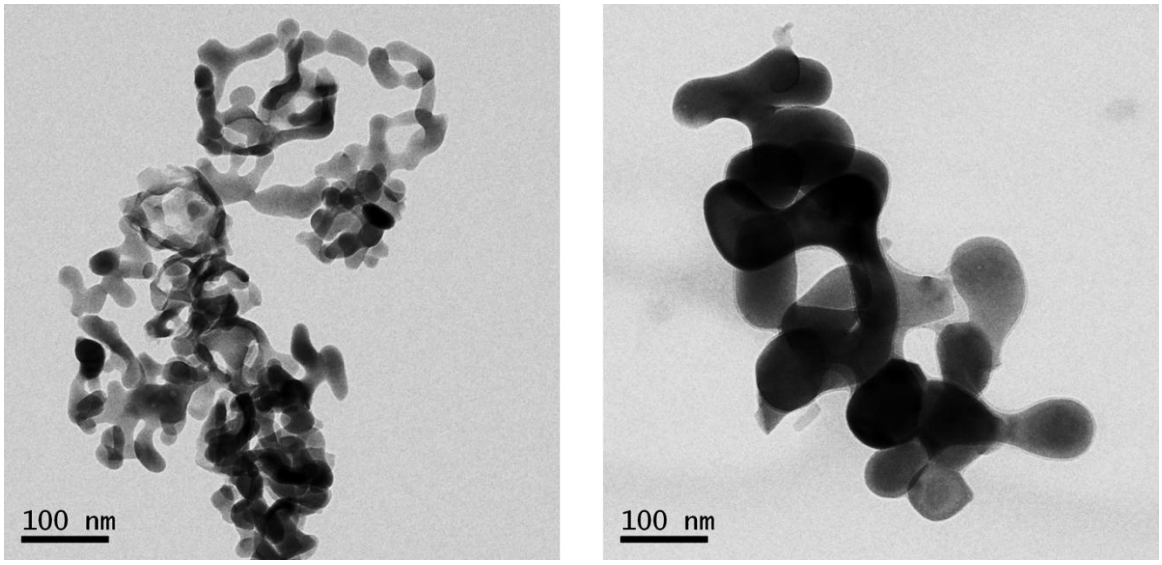

(a) (b)

Figure 4.12 TEM micrograph of YAG particles calcined at (a) 900 ^{o}C (b) 1100 ^{o}C.

It is clear from the micrograph that the particle size of the sample calcined at 900 ^{o} C is below 50 nm and that of calcined at 1100 ^{o} C is between 100-150 nm.

The morphology of the particles is somewhat In addition there is evidence of neck growth (initial stage of sintering) even at these low temperatures (900^{o}C) possibly due very fine particle size and consequent high surface area.

4.9 Energy dispersive spectroscopy (EDS) of the powder samples.

EDS gives us the information about elemental distribution of a sample by capturing the x-ray signals generated due to the interaction of electrons with the sample. As we know that stoichiometry is very important for achieving transparency in ceramics, the stoichiometry is calculated by the EDS data obtained. The following figure shows EDS intensity pattern.

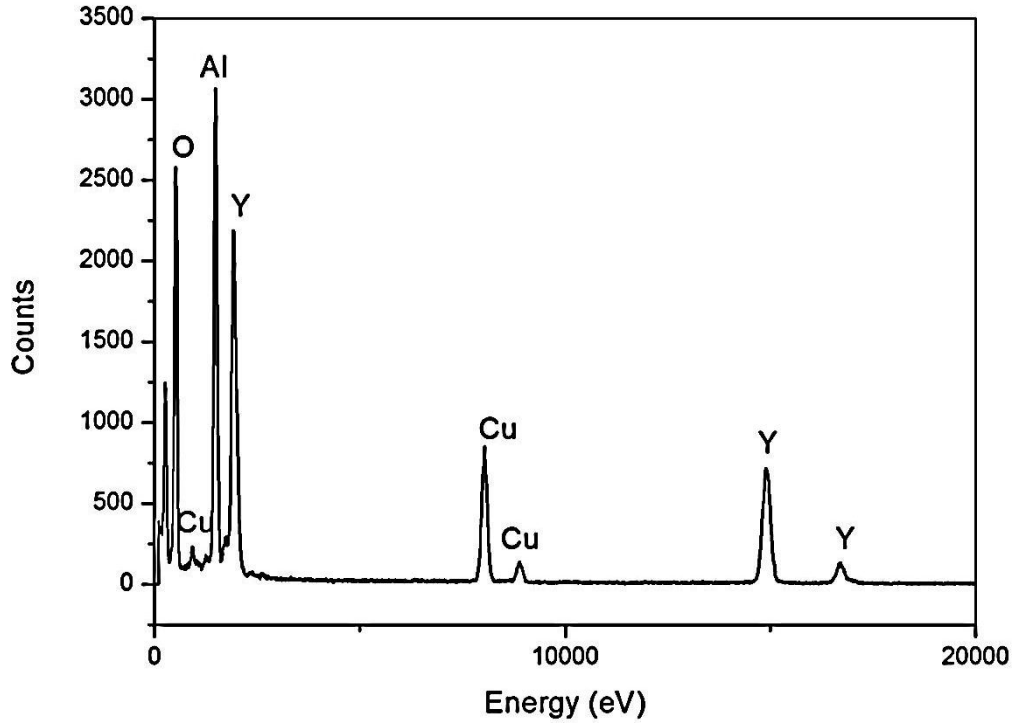

Figure 4.13 EDS pattern of YAG sample.

Element	Weight %	Atomic %
O(K)	30.99	58.67
Al(K)	22.79	25.58
Y(K	46.2	15.74

Y/Al ratio = 0.6153

There is a deviation of 0.01 from the ideal stoichiometry of Y/Al =0.61 for YAG ceramics.

Chapter 5

Processing and characterization of compacts

Chapter 5

Processing and characterization of compacts

5.1 Pre-compaction processing of nanopowders

The freeze dried powders are calcined at certain pre-decide temperature after which the powder is ground in an agate mortar to break down the local agglomerates. The powder is then blended with 1440 ppm of SiO_2 in the form of TEOS (tetra ethyl ortho silicate) diluted with ethanol. The blending was done for a long time to ensure proper homogeneity. Another set of powder were taken which was undoped. The blended powders were dried in an oven at 70 ^{o}C to remove the ethanol used for blending. Neodymium nitrate (1.4at% Nd) solution was added to silica doped YAG nanopowder for spark plasma sintering.

5.2 Compaction of powders into green pellet

The calcined nanopowder was passed through 350 mesh size for obtaining uniform granule size to attain better flowability and hence a better green density. The powders calcined at 900, 1000, 1100 ^{o} C were selected for compaction. Two sets of sample were made by doping silica in the form of TEOS (tetra ethyl ortho-silicate). The powders were then filled into a circular steel die and uniaxially pressed at around 150 MPa. The dwell time for pressing was 90 seconds. Consolidation of loose ceramic powders is done by applying uniaxial load within in a confined space into a die using a steel die and punch. During pressing of loose ceramic powders there are three steps in which we can classify the stages of compaction as rearrangement, deformation and fragmentation, these phenomenon can be graphically explained in the following figure:

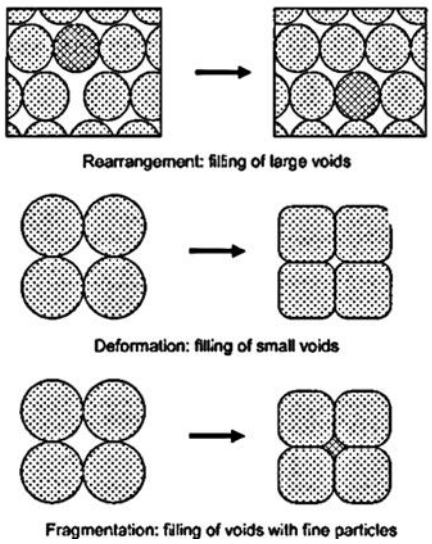

Figure 5.1 Schematic of the different stages of pressing of loose ceramic powder**.**

5.3 Characterisation of green pellets

Green densities of the pellets were calculated by dimensional method. Dimensions of the samples were measured using a digital Vernier caliper and corresponding weight were determined using an analytical balance. The calcination temperature, green densities along with sample dimensions are shown in Table 5.1 and the variation in density is shown in Figure 5.2.

Calcination temperature (^{o}C)	**Dimensions (mm)**		**Weight (g)**	**Green density (g/cc)**	**Average green density (%TD)**
	Diameter	**Thickness**			
900	12.07	5.02	0.886	1.54	33.91
1000	12.06	4.73	0.994	1.84	40.45
1100	12.07	3.61	0.847	2.05	45.09

Table 5.1 Calcination temperature, specimen dimensions and green density of the samples.

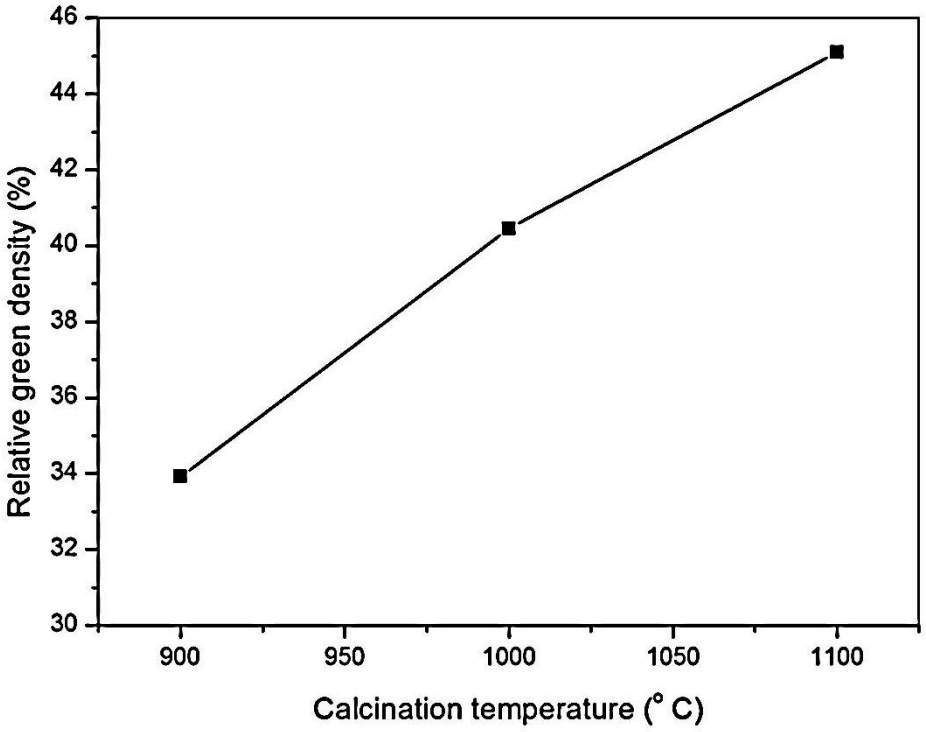

Figure 5.2 Dependence of green density of calcination temperature.

The powders are compacted without any addition of binder and the green strength is enough for handling. There is no requirement of binder because the powder is nanometric as a result surface area is huge due to which inter-particle friction is also large and it is this friction force that holds the structure together.

The probable reason for an increase in the green density with the increase in calcination temperature is the increase in particle size with temperature. A larger particle size has a lower surface area and hence the inter-particle friction is reduced facilitating easy particle sliding and rearrangement during pressing.

5.4 Sintering of the compacts

Sintering is a phenomenon of subjecting a pre-consolidated green body to high temperature below melting point. The driving force for sintering is the reduction in the total interfacial energy. The change in interfacial energy is because of surface area of the particles. Sintering is a competitive process of densification (removal of pores) and grain growth (coarsening of grains).

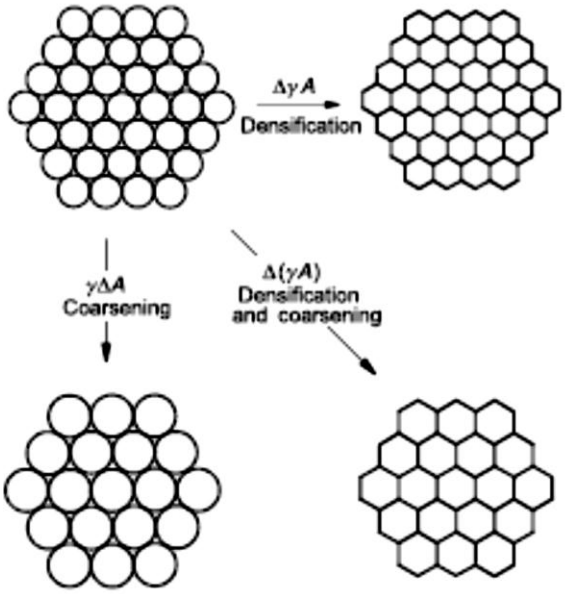

Figure 5.3 Schematic of the different stages of pressing of loose ceramic powder.

For achieving transparency in ceramics we need to attain very high density. Solid state sintering is mainly used for fabricating transparent ceramics because liquid phase sintering will need enough liquid which might possibly produce secondary phases in the grain boundary and be the reason for scattering the light and render the body opaque. A variety of sintering process is used for fabricating transparent ceramics such as hot isostatic pressing (HIP), sinter-HIP, high temperature controlled atmosphere sintering, spark plasma sintering (SPS), etc. Among all these pressure-less sintering and spark plasma sintering will be the focus of our discussion in this thesis.

5.4.1 Conventional ramp and hold sintering

The conventional ramp and hold sintering employs longer duration of dwell time at final temperature for the elimination of residual porosity and often results in abnormal grain growth. Fig. 5.4 represents the schematic of constant rate of heating (CRH) sintering profile. As was discussed by many investigators, the two processes of densification by pore closure and grain growth are competitive and depend on temperature and grain size. Assuming that surface and grain boundary diffusions dominate in nanocrystalline compacts, the corresponding rates of densification and grain growth during the intermediate and final stages of pressure-less sintering may be expressed respectively as:

$$\frac{1}{\rho}\frac{d\rho}{dt} \approx \frac{733 D_{gb}\delta_{gb}\gamma_{SV} V_m}{RTG^4\rho} \quad (1)$$

$$\frac{1}{G}\frac{dG}{dt} \approx \frac{110 D_S\delta_S\gamma_{gb} V_m}{RTG^4}(1-\rho)^{-\frac{4}{3}} \quad (2)$$

where D_{gb} and D_S are the diffusivities at the grain boundary and surface, δ_{gb} and δ_S are the grain boundary and surface thicknesses, where effective diffusion takes place, γ_{SV} and γ_{gb} are the specific surface and grain boundary energies, G is the grain size, ρ is the density, V_m is the molar volume, T is the absolute temperature, and R is the gas constant. Following equations (1) and (2) as was discussed by Rahaman and Kang et al., it is evident that under present assumptions the low sintering temperatures are preferred to keep the grain sizes low preserving the nanostructure during the densification. Further, at high temperatures the lattice diffusion dominates and grain growth occurs predominantly simultaneously with densification.

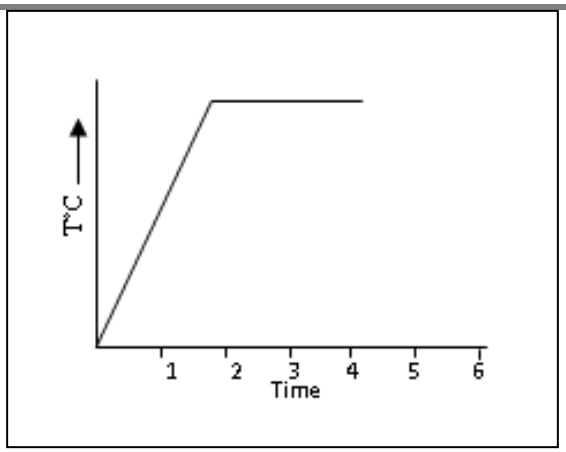

Figure 5.4 Schematic of CRH sintering.

As stated earlier, during sintering, grain growth is also active and this reduces the total interfacial energy. When grain boundaries and pores are displaced simultaneously grain growth is controlled either by the grain boundaries or by the pores. If grain growth is controlled by grain boundaries, the pore dragging effect on the grain boundary migration is negligible. If grain growth is controlled by pores, the displacement rate of a pore/grain boundary together is fixed by the displacement rate of the pore. When grain growth is controlled by grain boundaries, the matter displacement involved is the atomic migration from one grain towards another through the separating grain boundary. In the case of grain growth controlled by pores, matter displacement proceeds either by surface-diffusion at the pore surface, gas phase transport in the pore or bulk diffusion in the grains. The determination of the mechanisms controlling grain growth and densification during sintering of ceramics is not an easy task and most of the time results require critical analysis.

5.4.2 Spark Plasma Sintering (SPS)

Spark plasma sintering simultaneously applies pulsed electrical current and pressure directly on the sample leading to densification at relatively lower temperatures and short retention times. As both the die and sample are directly heated by the Joule effect extremely high

heating rates are possible due to which non-densifying mechanisms like surface diffusion can be surpassed.

The versatility of SPS allows very quick densification to near theoretical density for a number of metallic, ceramic and multi-layer materials under a low vacuum /inert environment. It is a novel hot pressing technique where very high heating rates upto (~ 500°C/min) were achieved by the application of pulsed electrical current and pressure (150MPa) simultaneously. In hot pressing, the precursor powder is loaded in a die and a uniaxial pressure is applied during the sintering. In the SPS technique, where a pulsed direct current is passed through an electrically conducting pressing die working as the heating element gives more rapid densification rate due to the use of pressure and rapid heating rate. The presence of a pulsed electrical field might create sparks during the initial part of the sintering, which clean the particles surface and thus facilitate grain boundary diffusion. Electrical field induced diffusion processes might also contribute to increased densification rate. Figure 5.5 shows a schematic of SPS setup.

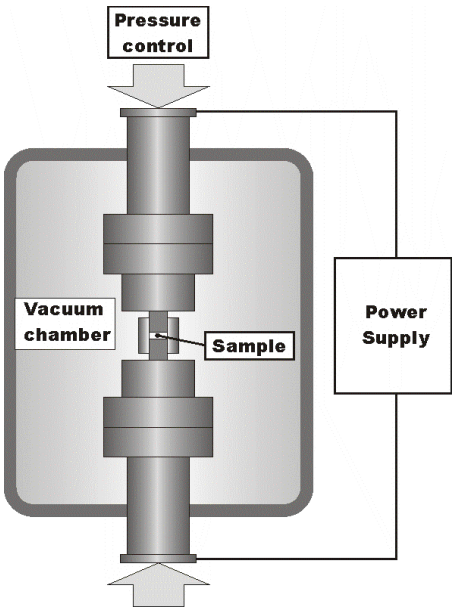

Figure 5.5 Schematic of spark plasma sintering furnace.

5.5 Conventional Sintering of Pellets in Laboratory Furnace

The green compacts were subjected to a temperature of 1650 ^{o}C at a constant heating rate of 3^{o} C/min for a soaking period of 6 hours in a PID (Libratherm) controlled lab furnace (Bysakh furnace).

5.6 Charecterization of sintered samples

The sintered samples were characterized for density using Archimedes principle. Microstructural analyses of polished and thermally etched samples were carried out using Scanning Electron Microscope (JEOL, 6480 LV).

5.7 Density characterisation of sintered samples

The powders calcined at 900, 1000, 1100 ^{o} C were doped with 1440 ppm of silica in the form of TEOS (tetra-ethyl orttho silicate) compacted and pressure-less sintered at 1650 ^{o} C for 6 hrs. The corresponding samples were also sintered without silica for the purpose of comparision.

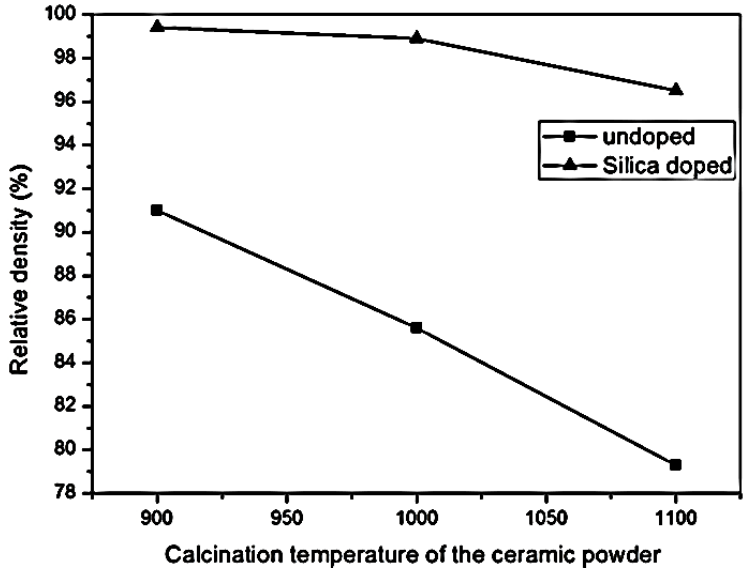

Figure 5.6 Dependence of sintered density on calcination temperature.

The enhanced densification is due to activated sintering in presence of silica as the inter-granular film which facilitates mass diffusion through the grain boundaries. Such high densification is suitable for obtaining transparency in ceramics but with pressure-less sintering it is not possible to remove the residual porosities residing within the grains (isolated pores).

5.8 Ceramographic specimen preparation for microstructural characterization

Ceramographic specimen preparation normally requires a specific sequence of operation such as sectioning, mounting, grinding, polishing and etching. Further to obtain an accurate interpretation of a microstructure the prepared specimen should be representative of the material being examined. The samples were coarse ground to remove deformation produced during sectioning and to make flat surface

5.9 Mounting and polishing

The samples were mounted in acrylate based resin moulds. An automatic grinding and polishing machine (Buehler, Ecomet) was used for grinding and polishing the sample. Mounted samples were placed in the sample holder and was ground using polishing disc of SiC grit size 120μm and number of revolutions were fixed at 250 per minute The ground samples were further polished using diamond suspensions of 5, 3, 1 μm particle size to achieve the required surface finish. The samples were cleaned and are examined under optical microscope for scratches, stains, and other imperfection. Polished samples were removed from the mount, cleaned with acetone and thermally etched at 1550 ^{o}C below the sintering temperature with soaking time of 30 minutes in a laboratory furnace.

5.10 Microstructural Analysis

The sintered samples were polished with varying grades of diamond slurry to obtain a mirror finish followed by thermal etching at 1550 ^{o}C to reveal the grain boundaries. The mcirostructure of the thermally etched samples were revealed in a scanning electron microscope. The micrographs of samples sintered from powders calcined at different temperature.

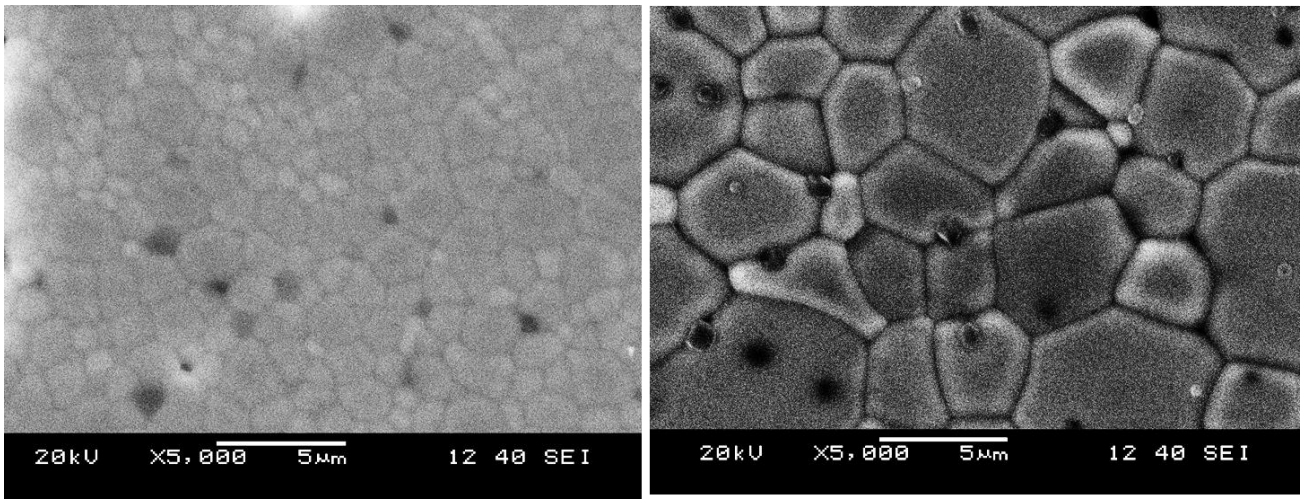

(a)9u **(b)9s**

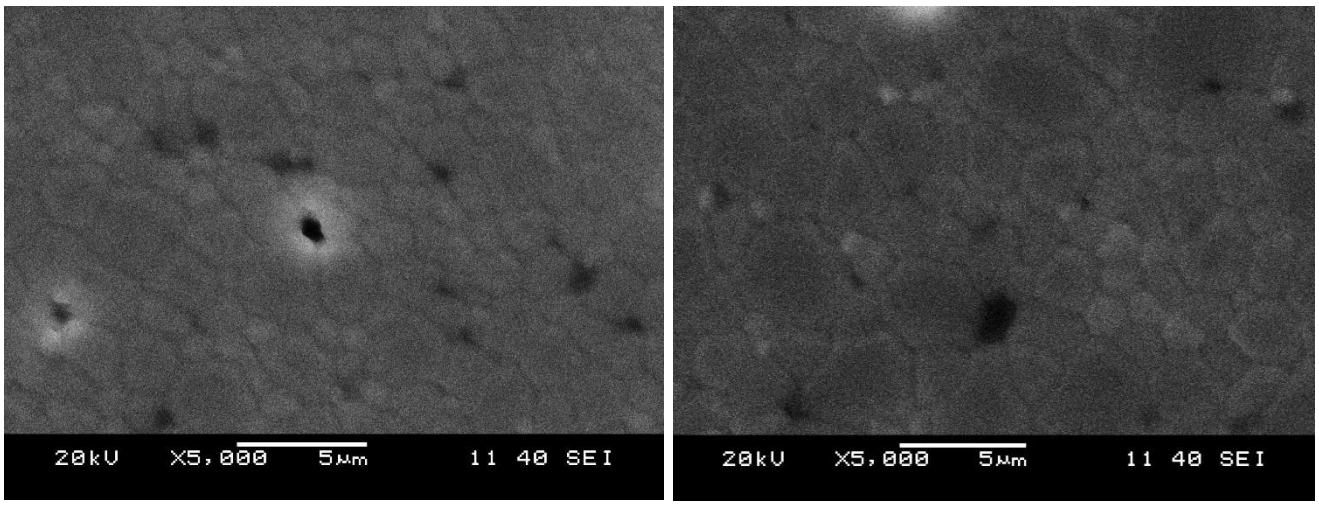

(c) 11u **(d) 11s**

Figure 5.7 SEM microstructure of samples calcined at (a) 900 ^{o}C and undoped, (b) 900 ^{o}C and doped with SiO_2, (c) 1000 ^{o}C and undoped**,** (d) 1000 ^{o}C and doped with SiO_2.

The microstructure of the samples calcined at 900 ^{o} C shows a finer grain size but the samples doped with silica have a larger grain size indicating the formation of an inter-granular film (IGF) due to which activated or transient liquid phase sintering has taken place enhancing the density further. In each microstructure there was normal grain growth rather than abnormal grain growth which is detrimental in case of transparent ceramics.

The electron images are nearly pore free suggesting very high density attained after sintering. The microstructure is equiaxed and the grain size of undoped sample is approximately 2 microns whereas the doped samples had a grain size of around 5 microns. The microstructure can be said as a stable one because the grains are more or less pentagons or hexagons which is more or less the equilibrium grain shape in two dimension.

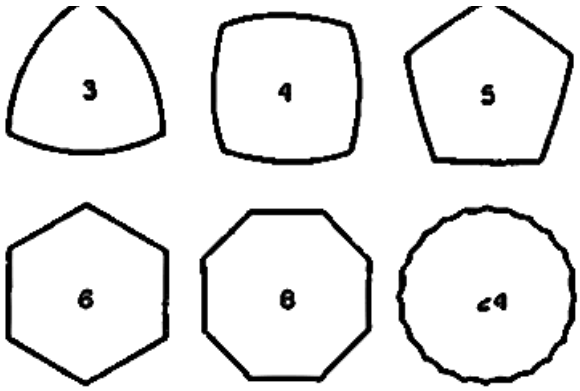

Figure 5.8 Curvature of sides of polygons correlated with grains in microstructure**.**

5.11 Spark plasma sintering of Nd:YAG nanopowder

The powders calcined at 900 ^{o} C doped with 1440 ppm of silica were selcted for spark plasma sintering, based on the density attained by pressure-less sintering. The powder was further doped with Nd_2O_3 (5 at.% Nd) in the form of neodynium nitrate (Alfa Aesar).The spark plasma sintering (Dr. Sinter Lab SPS Syntex) was done at 1300 and 1400 ^{o} C for 5 mins soaking time with an uniaxial loading of 62 MPa. Further the samples were annealed at 1000

^{o} C to get rid of the graphite contamination. The density of SPSed samples measured by archimedes method resulted in values close to theoretical density value.The following figure shows a sample of transparent 5 at.% Nd: YAG placed over printed text.

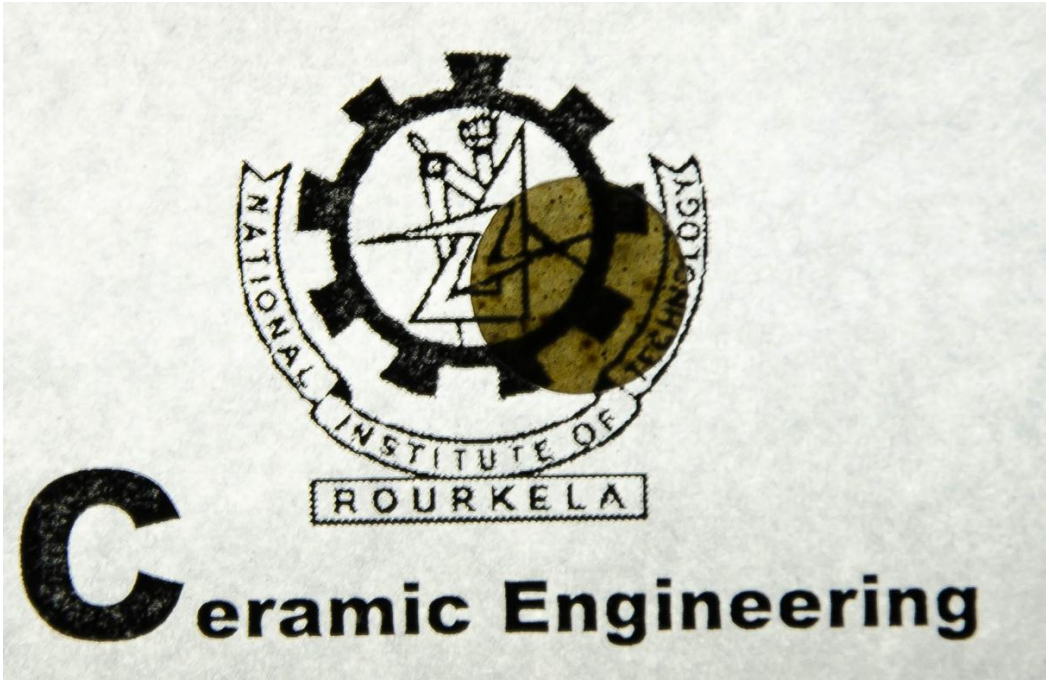

Figure 5.9 Image of SiO_2 doped Nd:YAG after SPS at 1300^{o}C.

5.12 Optical property evaluation of spark plasma sintered Nd:YAG ceramics

The mirror polished spark plasma sintered samples were analysed in a UV-VIS spectrophotometer for obtaining the absorption and transmission percentage. The sample was even analysed in an FTIR for transmission data in IR range. The optical transmission for a laser gain media is important because the pump lamp (xenon flash light) operates in a the optical frequency range and the lasing acttion takes place in the IR range (1064 nm). Hence the laser gain media must be transmitting in both the frequency range.

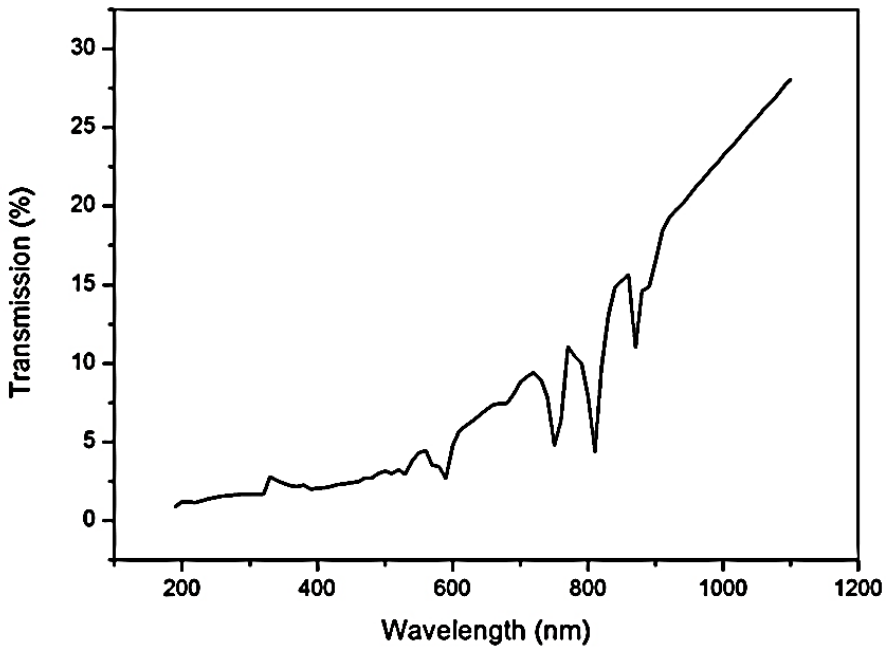

Figure 5.10 Transmission spectra of transparent SPSed YAG sample.

The transmittance is around 30 % (50 % of standard 5 at. % Nd: YAG) suggesting the possibility of lasing action at a wavelength of 1064 nm. The transmission at 550 nm is around 5 % which not adequate for lamp pumping action and hence it needs further investigation to enhance the transmission in optical range.

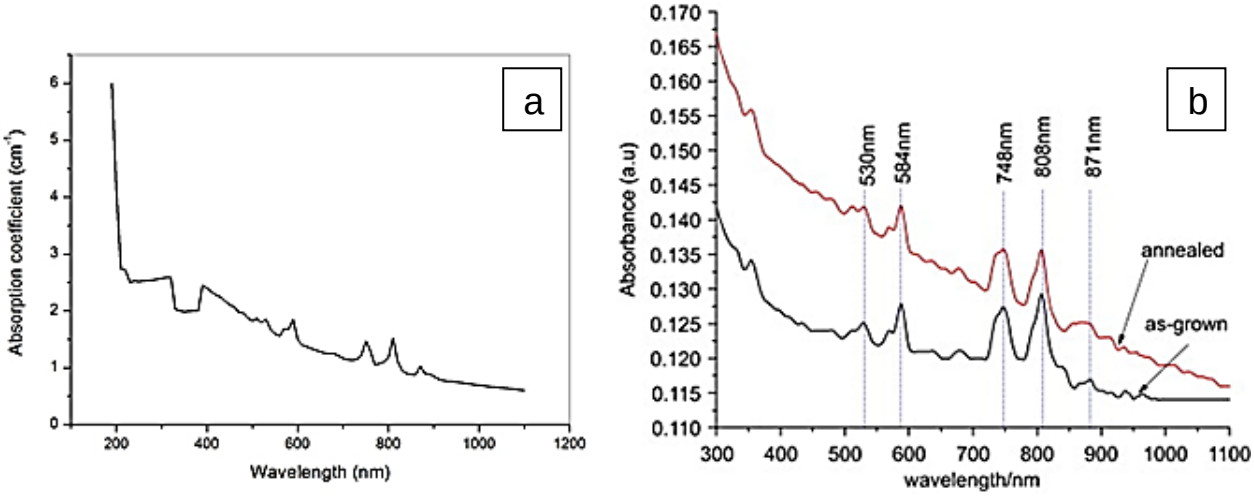

Figure 5.11 Absorbance pattern of transparent SPSed YAG sample.

The absorbance pattern is comparable with the standard absorbance data of as-grown YAG crystal. Figure 5.11a is experimental absorption pattern for spark plasma sintered specimens, whereas figure 5.11b represents the literature data.

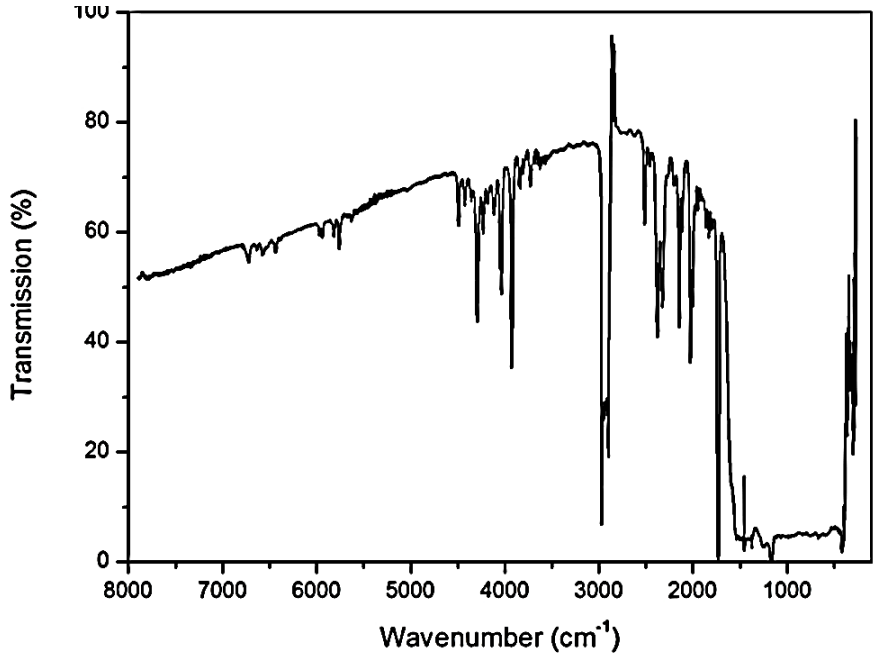

Figure 5.12 IR spectra of transparent SPSed YAG sample.

The transmission in the vicinity of 1100 nm is more than 50 % indicating the possibility of lasing action at a wavelength of 1064 nm.

Chapter 6

Conclusion

Conclusion

- A low temperature method was successfully implemented for the synthesis of Nano metric YAG ceramic powders having a very high surface area of 42 meter square per gram a particle size below 50 nm.
- A pressure–less sintered density of about 99 % was achieved by sintering at 1650 degree Celsius for 6 hrs.

- Transparent YAG samples were successfully fabricated by spark plasma sintering at 1300 degree Celsius for 5 minutes.
- This is the first successful attempt in this Institute to prepare transparent ceramics.
- This is also the first ever demonstration of the YAG powder processing technique to achieve transparent Nd doped YAG ceramics in this country.

References

[1] C. Greskovich et al., "Fabrication of Transparent ThO2-Doped Y_2O_3," Am. Ceram. Soc.Bull. 52 [5] 473-478 (1973).

[2] A.Krell et al., "Transparent compact ceramics: Inherent physical issues", Opt. Mat. 31 (2009) 1144–1150.

[3] R. Johnson et al. "Transapent polycrystalline ceramics: An overview", Trans. of the Indian Ceram. Soc. 71 [2] 73-85 (2012).

[4] T. Ikegami et al., "Fabrication of transparent yttria ceramics by the low temperature synthesis of yttrium hydroxide," J. Am. Ceram. Soc., 85[7] 1725-1729 (2002).

[5] R. L. Coble, "Transparent Alumina and Method of Preparation," U.S. Pat. No. 3026 210, 1962.

[6] C. Greskovich et al., "Polycrystalline ceramic lasers," J. Appl. Phys., 44[10] 4599-4606 (1973).

[7] A.Ikesue et al., "Ceramic laser materials," Nat Photonics, 2[12] 721-727 (2008).

[8] M. Katsurayama et al., Growth of Neodymium Doped $Y_3Al_5O_{12}$ Single Crystals by Double Crucible Method, J. Cryst. Growth, 229 [1] 193–8 (2001).

[9] A. Siegman, Lasers. University Science Books, Mill Valley, CA, 1986.

[10] Mizuno et al., Gept. Govt. Ind. Res. Inst. Nagoya, 16, 171 (1967).

[11] R. L. Coble, "Sintering Crystalline Solids. I. Intermediate and Final State Diffusion Models," J. Appl. Phys., 32 [5] 787 (1961).

[12] C. D. Greskovich et al., "Polycrystalline Ceramic Laser," Amer.Ceram. Soc. Bull., 51 [4] 324 (1972).

[13] A.Ikesue, "Polycrystalline Nd:YAG ceramics lasers," Opt. Mater., 19[1] 183-187 (2002).

[14] G. L. Messing et al., Method for manufacture of transparent ceramics, US Patent US-20090108507 – 7799267 (2009).

[15] C. Marlot et al., "Synthesis of YAG nanopowder by the co-precipitation method: Influence of pH and study of the reaction mechanisms",J. Of Solid State Chem. 191 (2012) 114–120 .

[16] X. Li et al., "Preparation of uniformly dispersed YAG ultrafine powders by co-precipitation method with SDS treatment" Powd. Tech. 196 (2009) 26–29 27.

[17] Y. Sang et al., "Chemical composition evolution of YAG co-precipitate determined by pH during aging period and its effect on precursor properties" Ceram. Int. 38 (2012) 1635–1641.

[18] J. Li et al.," Co-precipitation synthesis route to yttrium aluminium garnet (YAG) transparent ceramics", Jour. of the Eur. Ceram. Soc. 32 (2012) 2971–2979.

[19] S. Yang et al., "Nd:YAG nano-crystalline powders derived by combining co-precipitation method with citric acid treatment" Ceram. Int. 38 (2012) 3185–3189.

[20] Vrolijk et al. "Coprecipitation of Yttrium and Aluminium Hydroxide for Preparation of Yttrium Aluminium Garnet", J. of the Eur. Ceram. Soc. 6 (1990) 47-51.

[21] Q.X. Zheng et al., "Fabrication of YAG mono-dispersed particles with a novel combination method employing supercritical water process", J. of Supercritical Fluids 50 (2009) 77–81.

[22] M. Zeng, et al., "The effect of precipitant on co-precipitation synthesis of yttrium aluminiumgarnetpowders",Ceram.Int.(2012),http://dx.doi.org/10.1016/j.ceramint.2012.05.066.

[23] L. Wang 3764 et al., "The effect of precipitant concentration on the formation procedure of yttrium aluminium garnet (YAG) phase" Ceram Int. 38 (2012) 3763–3771.

[24] Y. Rabinovitch et al.' "Freeze-dried nanometric neodymium-doped YAG powders for transparent ceramics", J. of Mat. Proc. Tech. 199 (2008) 314–320.

[25] S. Kochawattana et al., "Sintering and grain growth in SiO_2 doped Nd:YAG" J. of the Eur. Ceram. Soc. 28 (2008) 1527–1534.

[26] Lee aet al., "Solid-State Reactive Sintering of Transparent Polycrystalline Nd:YAG Ceramics", J. Am. Ceram. Soc., 89 [6] 1945–1950 (2006).

[27] Yanagitani et al., "Neodymium doped yttrium aluminum garnet ($Y_3Al_5O_{12}$) nanocrystalline ceramics—A new generation of solid state laser and optical materials", J. of Al. and Com. 341, 220–225 (2002).

[28] R. Chaim et al., "Transparent YAG ceramics by surface softening of nanoparticles in spark plasma sintering", Mat. Sc. and Engg A 429, 74–78 (2006).

[29] Y Tanget al., "Sintered Polycrystalline Yttrium Aluminum Garnet and use thereof in Optical Devices", US Patent, US2010/0048378-A1 (2010).

[30] M. Suárez et al., "Hot isostatic pressing of optically active Nd:YAG powders doped by a colloidal processing route", Jour. of the Eur. Ceram. Soc. 30, 1489–1494 (2010).

[31] S. Ramanathan et al., "Transparent YAG from powder prepared by homogeneous precipitation reaction—$Al(NO_3)_3$+$Y(NO_3)_3$+$(NH_4)_2SO_4$+$CO(NH_2)_2$ ", J. Mat. Sc. Letters 20 [23] 2119 – 2121 (2001).

[32] S. Bhattacharyya et al., "Pressurless reaction sintering of yttrium aluminium garnet (YAG) from powder precursor in the hydroxyhydrogel form", Ceram. Int., 2011(Article in Press)

[33] R. Singh et al.," Preparation and characterization of nanocrystalline Nd-YAG powder", Mat. Lett., 61 [3] 921-924 (2007).

[34] R. Choudhary et al., Rapid synthesis of Nd:YAG nanopowder by microwave flash combustion, Materials Science-Poland, 27, 4/1 (2009).